Supporting Information

Catenated Nitrogen-Rich Triazine-Tetrazole Molecules for Advanced Explosives and Gas-Generator Applications

Manojkumar Jujam,[a] Vikas D. Ghule,[b] Srinivas Dharavath[a]*

[a]Energetic Materials Laboratory, Department of Chemistry, Indian Institute of Technology Kanpur, Kanpur-208016, Uttar Pradesh, India. orcid.org/ 0000-0003-0511-0607. E-mail: srinivasd@iitk.ac.in

[b]Department of Chemistry, National Institute of Technology Kurukshetra, Kurukshetra-136119, Haryana, India.

Table of Contents

General Methods and synthesis of compounds S2-S5

Crystal description of compound **5** S6-S10

Crystal description of compound **8** S11-S14

Copies of ^{1}H and ^{13}C{^{1}H} spectra, and IR plots for **3** S15-S16

Copies of ^{1}H and ^{13}C{^{1}H} spectra, HRMS and IR plots for **4** S16-S18

Copies of ^{1}H, ^{13}C{^{1}H}, ^{15}N spectra, IR, and DSC plots for **5** S18-S21

Copies of ^{1}H, ^{13}C{^{1}H} spectra, IR, and HRMS plots for **7** S21-S23

Copies of ^{1}H and ^{13}C{^{1}H} spectra, IR, HRMS, and DSC plots for **8** S23-S25

Copies of ^{1}H, and ^{13}C{^{1}H} spectra for **9I** S26-S26

^{15}N NMR of **5**, Mechanism of **8**, Hirshfeld surface of **5** and **8**, S27-S29

ESP Plots, Hot needle test of **8** and Computation details S29-S35

Combustion details of **5**, **8** and **NaN$_3$** S36-S43

References S43-S44

Experimental Section:

Caution! The compounds in this work are energetic materials that could potentially explode under certain conditions (e.g., impact, friction, or electric discharge). Appropriate safety precautions, such as the use of shields in a fume hood and personal protection equipment (safety glasses, face shields, ear plugs, as well as gloves) should be always taken when handling these materials.

General. All reagents were purchased from AKSci or TCI or Merck in analytical grade and were used as supplied. ^{1}H, ^{13}C{^{1}H}, and ^{15}N NMR spectra were recorded JEOL DELTA (ECS) 400 (^{1}H, 400 MHz) and ^{13}C{^{1}H} NMR (100 MHz, DMSO-d_6) nuclear magnetic resonance spectrometer. Chemical shifts for ^{1}H NMR and ^{13}C{^{1}H} NMR spectra are given with respect to external $(CH_3)_4Si$ (^{1}H and ^{13}C). [D6] DMSO was used as a locking solvent unless otherwise stated. IR spectra were recorded using Zn-Se pellets with a ECO-ATR spectrometer (Bruker Alpha II). A single crystal of suitable dimensions was used for data collection. Diffraction intensities were collected on a Bruker APEX-II CCD diffractometer, with graphite-monochromated Mo Kα (0.71073 Å) radiation at 100(2) K. Density was determined at room temperature by employing Anton Par Ultra5000 gas pycnometer. Decomposition temperatures (onset) were recorded using a dry nitrogen gas purge and a heating rate of 5 °C min^{-1} on a thermogravimetric differential scanning calorimeter (TGA-DSC (SDT-650)). HRMS was recorded on a Quadrupole Time-of-Flight Mass Spectrometry mass spectrometer and ESI-MS was recorded on Agilent mass spectrometer. Impact and friction sensitivity measurements were made using a standard BAM fall hammer and a BAM friction tester.

Synthesis of 2-amino-6-chloropyridine-3,5-dicarbonitrile (2): Compound **2** was synthesized using previously reported literature procedure[4]. A mixture of malononitrile (5 g, 75.69 mmol, 2 equiv.), triethyl orthoformate (5.61 g, 37.84 mmol, 1 equiv.) and pyridine (2.99 g, 37.84 mmol, 1 equiv.) was allowed to reflux for 20 minutes, to this con HCl was added at 80 °C, cooled to room temperature, and water (20 ml) was added in to it. The newly formed precipitate was collected by filtration, washed with water, ethanol and diethyl ether to afford the intermediate 2-amino-6-chloropyridine-3,5-dicarbonitrile (9.74 g, 96%, 0.05 mmol).

Synthesis of 2,6-diaminopyridine-3,5-dicarbonitrile (3): Compound **2** (1.000 g, 0.0056 mol) was dissolved in acetonitrile (5 mL) in a pressure tube and aqueous ammonia (5 mL excess) was added in it and the reaction was stirred at 90 °C for 15 hours. After cooling down to room temperature, newly formed light yellowish-brown coloured precipitate was filtered off and washed with acetonitrile and cold water, dried under vacuum to afford compound **3** in 79% yield (0.71 g, 0.0044 mol). ^{1}H NMR (400 MHz, DMSO-d$_6$): δ 8.02 (s, 1H), 7.20 (s, 4H). ^{13}C{^{1}H} NMR (100 MHz, DMSO-d$_6$) δ 79.2, 117.3, 148.7, 161.2 ppm. IR (ATR ZnSe): 3427, 3348, 3149, 2208, 1671, 1636, 1592, 1538, 1468, 1262, 1097, 932, 766, 705 cm^{-1}. Elemental Analysis Calcd for $C_7H_5N_5$, (0.2 CH_3OH) C, 52.23; H, 3.53; N, 42.30. Found: C, 51.90; H, 3.27; N, 42.78.

Synthesis of 3-(1H-tetrazol-5-yl)-5-(2H-tetrazol-5-yl)pyridine-2,6-diamine (4): Compound **3** (0.5000 g, 0.0031 mol) was dissolved in N, N-dimethyl formamide (DMF) (5 mL). To this, sodium azide (NaN_3) (1.00 g, 0.0153 mol, 5 eq), and ammonium chloride (0.82 g, 0.015 mol, 5 eq) were added under a nitrogen atmosphere. The reaction mixture was stirred at 125 °C for 48 hours cooled to room temperature and the solvent was evaporated under reduced pressure. To this, ice-cold water was added and the pH was adjusted to 3-4 with diluted HCl. The newly formed creamy coloured precipitate was collected by filtration and washed with ice-cold water, dried under vacuum to afford compound **4** in 75% yield (0.58 g, 0.0023 mol).^{1}H NMR (400 MHz, DMSO-d$_6$): δ 8.53 (s, 1H), 7.34 (s, 4H). ^{13}C{^{1}H} NMR (100 MHz, DMSO-d$_6$) δ 91.7, 137.8, 155.0, 157.1 ppm. IR (ATR ZnSe): 3425, 3307, 3141, 1683, 1645, 1465, 1417, 1306, 1259, 1157, 10995, 1008, 948, 900, 765, 723, 660, 619 cm^{-1}. Elemental Analysis Calcd for $C_7H_7N_{11}$ (H_2O + 0.25 DMF): C, 33.07; H, 3.85; N, 55.98; Found: C, 32.68; H, 3.62; N, 55.92. HRMS (ESI-QTOF) m/z: $(M+H)^+$ Calcd for $C_7H_8N_{11}$ 246.0959; Found 246.0957.

Synthesis of 4-azido-7-oxo-6-(1H-tetrazol-5-yl)-7,8-dihydropyrido[2,3-d][1,2,3]triazine 2-oxide (5): In a 50 mL round-bottom flask, a mixture of KNO_3 (0.300 g) and the 98% sulphuric acid (4 mL) was added at room temperature. To this solution, compound **4** (0.300 g, 0.0012 mol) was added gradually, and the reaction mixture was stirred at room temperature for 15 hours and quenched with ice-cold water. The newly formed orange coloured precipitate was collected by filtration and washed with ice-cold water, dried under vacuum to afford compound **5** in 63% yield (0.334 g, 0.0012 mol).^{1}H NMR (400 MHz, DMSO-d_6): δ 8.45 (s, 1H). ^{13}C{^{1}H} NMR (100 MHz, DMSO-d_6) δ 94.0, 117.4, 131.0, 149.2, 156.2, 160.1, 160.4. ^{15}N NMR (500 MHz, DMSO-d_6): 12.0, -48.8, -92.7, -130.1, -139.4, 146.8, -152.4, -198.6, -229.2, -278.4 ppm. IR (ATR ZnSe): 3573, 3507, 2242, 2166, 1670, 1621, 1596, 1559, 1505, 1458, 1423, 1383, 1340, 1249, 1210, 1134, 1102, 1094, 1076, 1031, 966, 877, 831, 779, 726, 699, 646 cm^{-1}. Elemental Analysis Calcd for $C_7H_3N_{11}O_2$ (0.4 DMSO): C, 30.77; H, 1.79; N, 50.61; Found: C, 30.94; H, 2.10; N, 50.99. HRMS (ESI-QTOF) m/z: $(M-2H)^-$ Calcd for $C_7HN_{11}O_2$ 271.0326; Found 271.0444.

Synthesis of 2-(aminomethylene)malononitrile (6)^{5}: Compound **6** was synthesized from previously reported procedures using commercially available 2-(Ethoxymethylene)malononitrile (1.000 g, 0.0081 mol) was treated with aqueous ammonia (5 mL) in methanol (8 mL), and stirred at room temperature overnight. The solvent was evaporated under reduced pressure. The crude was dissolved in cold methanol, and the newly formed yellow coloured precipitate was collected by filtration and washed with ice-cold water and dried under vacuum to afford compound **6** in 68% yield (0.52 g, 0.0055 mol).

Synthesis of (Z)-3-amino-2-(1H-tetrazol-5-yl)acrylonitrile and 2,2-di(1H-tetrazol-5-yl)ethen-1-amine (7M): Compound **6** (1.00 g, 0.010 mol) was dissolved in water (20 mL), and to this NaN_3 (1.53 g, 0.023 mol) and Zinc chloride ($ZnCl_2$) (2.99 g, 0.022 mol) were added and refluxed for 15 hours and cooled to room temperature, and the pH was adjusted to 2-3 with concentrated HCl. The newly formed yellowish-green coloured precipitate was collected by filtration and washed with ice-cold water, dried under vacuum to afford compound **7M** in 66% yield (2.2 g, 0.0069 mol).^{1}H NMR (400 MHz, DMSO-d_6): δ 1.29 (t, 6H), 4.56 (q, 4H). ^{13}C{^{1}H} NMR (100 MHz, DMSO-d_6) δ 13.8, 67.2, 113.9, 132.8, 148.6, 151.6, 156.6. IR (ATR ZnSe): 3593, 3123, 2920, 2853, 1766, 1722, 1581, 1508, 1434, 1334, 1298, 1236, 1161, 1083, 999, 958, 901, 836, 799, 738 cm^{-1}. HRMS (ESI-QTOF) m/z: $(M-H)^-$ Calcd for $C_4H_4N_6$ 135.0425; Found 135.0419. $(M-H)^-$ Calcd for $C_4H_5N_9$ 178.0595; Found 178.0586. $(M-H)^-$ Calcd for $C_7H_5N_{13}$ 270.0695; Found 270.0718.

Synthesis of 6-azido-4-(2H-tetrazol-5-yl)tetrazolo[1',5':1,6]pyrido[2,3-d][1,2,3]triazine 8-oxide (8): In a 50 mL round-bottom flask, the 98% sulphuric acid (4 mL) and 100% HNO_3 (2 mL) were added at 0 °C. To this solution, compound **7M** (0.500 g, 0.0015 mol) was added slowly, and the reaction mixture was stirred at room temperature for 15 hours and quenched with ice-cold water. The newly formed yellow coloured precipitate was collected by filtration and washed with ice-cold water, dried under vacuum to afford compound **4** in 63% yield (0.30 g, 0.0010 mol).^{1}H NMR (400 MHz, DMSO-d_6): δ 1.29 (t, 6H), 4.56 (q, 4H). ^{13}C{^{1}H} NMR (100 MHz, DMSO-d_6) δ 13.8, 67.2, 113.9, 132.8, 148.6, 151.6, 156.6. IR (ATR ZnSe): 3593, 3123, 2920, 2853, 1766, 1722, 1581, 1508, 1434, 1334, 1298, 1236, 1161, 1083, 999, 958, 901, 836, 799, 738 cm^{-1}. Elemental Analysis Calcd for $C_7H_2N_{14}O$ (0.5 CH_3OH) C, 28.67; H, 1.28; N, 62.41; Found: C, 28.46; H, 1.42; N, 62.39. HRMS (ESI-QTOF) m/z: $(M+Na)^+$ Calcd for $C_7H_2N_{14}O$ 321.0434; Found 321.0432.

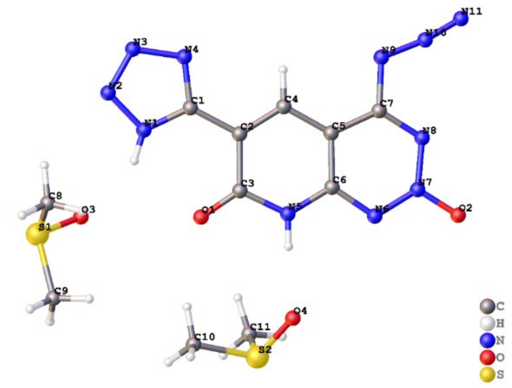

Figure S1: Molecular structure of compound **5**.

SHFSU01_ALERT_2_A The absolute value of the parameter shift to su ratio > 0.20. Absolute value of the parameter shift to su ratio given 0.415. Additional refinement cycles may be required.

Author Response: This is due to the disordered guest.

PLAT080_ALERT_2_A Maximum Shift/Error .... 0.41 Why ?

Author Response: This is due to the disordered guest.

Table S1: Crystal data and structure refinement for 5.

CCDC Number	2498162
Empirical formula	$C_{11}H_{13}N_{11}O_4S_2$
Formula weight	427.430
Temperature/K	100
Crystal system	triclinic
Space group	P-1
a/Å	5.1200(6)
b/Å	13.3302(16)
c/Å	13.9482(17)
α/°	80.226(4)
β/°	88.777(4)
γ/°	80.059(4)
Volume/Å^3	924.04(19)
Z	2
ρ_{calc}g/cm^3	1.536
μ/mm^{-1}	0.334
F(000)	440.7
Crystal size/mm^3	0.125 × 0.12 × 0.1
Radiation	Mo Kα (λ = 0.71073)
2Θ range for data collection/°	4.68 to 56.64
Index ranges	$-6 \le h \le 6$, $-17 \le k \le 17$, $-18 \le l \le 18$

Reflections collected	15046
Independent reflections	4585 [R_{int} = 0.0368, R_{sigma} = 0.0379]
Data/restraints/parameters	4585/0/265
Goodness-of-fit on F^2	1.059
Final R indexes [I>=2σ (I)]	R_1 = 0.0383, wR_2 = 0.1079
Final R indexes [all data]	R_1 = 0.0452, wR_2 = 0.1163
Largest diff. peak/hole / e Å^{-3}	0.50/-0.58

Table S2: Fractional Atomic Coordinates (×10^4) and Equivalent Isotropic Displacement Parameters (Å^2×10^3) for 5. U_{eq} is defined as 1/3 of of the trace of the orthogonalised U_{IJ} tensor.

Atom	*x*	*y*	*z*	U(eq)
S2	10538.8(8)	5056.2(3)	6595.4(3)	17.83(12)
S1	2968.8(9)	6786.6(4)	10141.9(3)	23.60(12)
O4	9978(2)	6067.2(9)	5877.2(9)	19.5(3)
O1	4195(2)	7115.3(10)	7044.8(9)	20.2(3)
O2	7229(2)	7323.5(10)	2292.8(9)	22.1(3)
O3	2152(3)	6630.2(11)	9154.8(10)	29.9(3)
N6	6321(3)	7296.2(11)	3847.3(10)	16.7(3)
N10	-1079(3)	9366.1(11)	2020.5(11)	19.4(3)
N7	5614(3)	7617.0(11)	2916.9(10)	16.9(3)
N5	5196(3)	7283.5(11)	5443.1(10)	15.3(3)
N9	-723(3)	9203.3(11)	2933.1(10)	17.9(3)
N8	3334(3)	8230.6(11)	2574.8(10)	16.9(3)
N1	-317(3)	8176.6(12)	7678.8(11)	19.4(3)
N4	-2952(3)	9196.6(11)	6596.9(11)	18.5(3)
N3	-3928(3)	9245.7(12)	7503.0(11)	22.2(3)
N2	-2360(3)	8634.1(13)	8161.2(11)	23.1(3)
N11	-1703(3)	9573.7(13)	1237.0(11)	27.2(4)
C1	-681(3)	8526.7(12)	6724.1(12)	15.7(3)
C2	1070(3)	8238.6(12)	5942.4(12)	14.9(3)
C5	2121(3)	8297.0(12)	4246.0(12)	14.8(3)
C3	3554(3)	7508.5(12)	6207.5(12)	15.0(3)
C7	1653(3)	8563.3(12)	3241.4(12)	15.7(3)
C6	4529(3)	7631.4(12)	4497.1(12)	14.1(3)
C4	402(3)	8612.1(12)	4995.0(12)	15.2(3)
C11	8018(3)	4350.2(14)	6385.6(15)	23.4(4)
C10	9474(4)	5353.5(15)	7754.7(14)	28.2(4)
C8	3079(5)	8128.6(16)	10039.1(15)	31.2(4)
C9	6443(4)	6321.3(19)	10237.2(18)	37.2(5)

Table S3: Anisotropic Displacement Parameters (Å^2×10^3) for 5. The Anisotropic displacement factor exponent takes the form: $-2\pi^2[h^2a^{*2}U_{11}+2hka^*b^*U_{12}+\ldots]$.

Atom	U_{11}	U_{22}	U_{33}	U_{12}	U_{13}	U_{23}

S2	11.10(19)	14.2(2)	27.1(2)	-0.94(14)	-2.90(15)	-1.42(16)
S1	23.2(2)	27.7(2)	18.0(2)	-4.40(18)	-2.68(16)	1.85(17)
O4	15.7(5)	16.4(6)	24.7(6)	-1.4(4)	-2.2(5)	0.3(5)
O1	17.8(6)	23.8(6)	16.3(6)	0.8(5)	-2.1(5)	0.4(5)
O2	20.8(6)	25.6(6)	19.4(6)	0.4(5)	4.2(5)	-7.2(5)
O3	34.1(8)	32.6(8)	21.9(7)	-3.6(6)	-9.9(6)	-1.8(6)
N6	16.6(6)	16.4(7)	16.6(7)	-1.8(5)	-1.1(5)	-2.5(5)
N10	19.4(7)	17.7(7)	18.8(7)	1.9(6)	-0.6(6)	-1.8(5)
N7	16.9(6)	16.6(7)	17.5(7)	-2.7(5)	1.1(5)	-4.0(5)
N5	12.3(6)	16.0(6)	16.3(7)	-0.1(5)	-2.0(5)	-1.2(5)
N9	18.4(7)	18.8(7)	14.7(6)	1.1(5)	-2.6(5)	-1.7(5)
N8	16.2(6)	16.1(6)	17.4(7)	-0.7(5)	-1.9(5)	-1.8(5)
N1	16.1(7)	23.2(7)	17.8(7)	0.6(6)	-0.9(6)	-4.5(6)
N4	16.4(7)	18.3(7)	19.8(7)	0.5(5)	0.1(5)	-3.4(6)
N3	19.6(7)	25.5(8)	20.5(7)	0.5(6)	1.3(6)	-5.8(6)
N2	19.6(7)	28.4(8)	20.0(7)	1.1(6)	1.1(6)	-6.1(6)
N11	30.5(8)	27.5(8)	18.9(8)	5.0(7)	-2.6(6)	-0.6(6)
C1	14.5(7)	15.0(7)	17.9(8)	-2.7(6)	-1.4(6)	-3.2(6)
C2	13.2(7)	13.5(7)	18.1(8)	-2.6(6)	-1.4(6)	-2.5(6)
C5	14.9(7)	13.3(7)	16.4(7)	-3.2(6)	-2.2(6)	-2.0(6)
C3	12.9(7)	14.8(7)	17.7(7)	-2.7(6)	-1.0(6)	-3.5(6)
C7	16.1(7)	12.7(7)	18.1(8)	-2.7(6)	-1.3(6)	-1.7(6)
C6	13.9(7)	11.8(7)	17.2(8)	-3.4(6)	0.0(6)	-3.1(6)
C4	14.5(7)	12.8(7)	18.0(8)	-2.1(6)	-2.0(6)	-1.9(6)
C11	16.6(8)	21.8(8)	33.1(10)	-6.6(7)	-0.3(7)	-5.2(7)
C10	38.0(11)	23.3(9)	20.8(9)	0.9(8)	-9.3(8)	-1.4(7)
C8	43.3(12)	25.9(10)	22.4(9)	0.8(9)	1.7(8)	-4.9(8)
C9	27.2(10)	39.4(12)	44.9(13)	5.6(9)	-13.6(9)	-16.5(10)

Table S4: Bond Lengths for 5.

Atom	Atom	Length/Å	Atom	Atom	Length/Å
S2	O4	1.5239(12)	N5	C6	1.353(2)
S2	C11	1.7795(18)	N9	C7	1.390(2)
S2	C10	1.782(2)	N8	C7	1.333(2)
S1	O3	1.5053(14)	N1	N2	1.345(2)
S1	C8	1.781(2)	N1	C1	1.340(2)
S1	C9	1.780(2)	N4	N3	1.357(2)
O1	C3	1.223(2)	N4	C1	1.333(2)
O2	N7	1.2523(18)	N3	N2	1.305(2)
N6	N7	1.3327(19)	C1	C2	1.456(2)
N6	C6	1.350(2)	C2	C3	1.474(2)
N10	N9	1.266(2)	C2	C4	1.360(2)
N10	N11	1.120(2)	C5	C7	1.401(2)
N7	N8	1.3495(19)	C5	C6	1.402(2)

N5	C3	1.384(2)	C5	C4	1.423(2)

Table S5: Bond Angles for 5.

Atom	Atom	Atom	Angle/°	Atom	Atom	Atom	Angle/°
C11	S2	O4	105.74(8)	C2	C1	N1	126.82(15)
C10	S2	O4	106.51(8)	C2	C1	N4	124.74(15)
C10	S2	C11	98.35(10)	C3	C2	C1	118.05(14)
C8	S1	O3	106.11(9)	C4	C2	C1	120.98(14)
C9	S1	O3	105.82(10)	C4	C2	C3	120.95(15)
C9	S1	C8	97.88(11)	C6	C5	C7	113.89(15)
C6	N6	N7	115.08(13)	C4	C5	C7	126.70(15)
N11	N10	N9	171.20(17)	C4	C5	C6	119.40(15)
N6	N7	O2	116.91(14)	N5	C3	O1	120.36(14)
N8	N7	O2	116.37(14)	C2	C3	O1	123.62(15)
N8	N7	N6	126.73(14)	C2	C3	N5	116.02(14)
C6	N5	C3	123.47(14)	N8	C7	N9	118.77(15)
C7	N9	N10	114.02(14)	C5	C7	N9	117.42(15)
C7	N8	N7	116.12(14)	C5	C7	N8	123.81(15)
C1	N1	N2	108.71(14)	N5	C6	N6	115.43(14)
C1	N4	N3	105.56(14)	C5	C6	N6	124.33(15)
N2	N3	N4	110.92(14)	C5	C6	N5	120.23(15)
N3	N2	N1	106.37(14)	C5	C4	C2	119.73(15)
N4	C1	N1	108.43(15)				

Table S6: Torsion Angles for 5.

A	B	C	D	Angle/°	A	B	C	D	Angle/°
O1	C3	N5	C6	175.13(15)	N5	C6	C5	C7	-177.80(15)
O1	C3	C2	C1	1.64(19)	N5	C6	C5	C4	0.71(18)
O1	C3	C2	C4	-176.76(16)	N9	C7	C5	C6	178.61(15)
O2	N7	N6	C6	179.83(14)	N9	C7	C5	C4	0.22(19)
O2	N7	N8	C7	-178.26(14)	N8	C7	C5	C6	-0.70(18)
N6	N7	N8	C7	1.48(18)	N8	C7	C5	C4	-179.09(15)
N6	C6	N5	C3	-177.01(13)	N1	N2	N3	N4	0.09(16)
N6	C6	C5	C7	2.46(18)	N1	C1	N4	N3	0.54(15)
N6	C6	C5	C4	-179.03(16)	N1	C1	C2	C3	-1.8(2)
N10	N9	C7	N8	3.01(17)	N1	C1	C2	C4	176.58(17)
N10	N9	C7	C5	-176.33(14)	N4	C1	C2	C3	178.20(16)
N7	N8	C7	N9	179.61(14)	N4	C1	C2	C4	-3.4(2)

N7	N8	C7	C5	-1.09(17)	C1	C2	C4	C5	-178.45(15)
N5	C3	C2	C1	-177.94(14)	C2	C4	C5	C7	176.15(15)
N5	C3	C2	C4	3.66(17)	C2	C4	C5	C6	-2.16(18)

Table S7: Hydrogen Atom Coordinates (Å×10⁴) and Isotropic Displacement Parameters (Å²×10³) for 5.

Atom	*x*	*y*	*z*	U(eq)
H4	-1207(3)	9081.6(12)	4833.8(12)	18.2(4)
H11a	6273(3)	4774(4)	6440(11)	35.0(6)
H11b	8214(18)	4171(10)	5732(4)	35.0(6)
H11c	8177(18)	3717(6)	6870(7)	35.0(6)
H10a	10668(19)	5764(11)	7985(5)	42.3(6)
H10b	7667(13)	5749(11)	7698(3)	42.3(6)
H10c	9500(30)	4710.9(15)	8218(3)	42.3(6)
H8a	4290(20)	8329(3)	9517(8)	46.9(7)
H8b	1299(7)	8528.3(17)	9889(12)	46.9(7)
H8c	3710(30)	8267(3)	10655(4)	46.9(7)
H9a	6782(5)	5573(3)	10250(13)	55.8(8)
H9b	7335(6)	6660(10)	9676(7)	55.8(8)
H9c	7127(7)	6474(12)	10838(7)	55.8(8)
H1	860(60)	7750(20)	7990(20)	42(7)
H5	6640(50)	6860(20)	5588(18)	36(7)

Figure S2: Molecular structure of Compound **8**.

Table S8: Crystal data and structure refinement for 8.

CCDC No.	2498161
Empirical formula	$C_{14}H_2N_{28}O_2$
Formula weight	594.44
Temperature/K	100.0

Crystal system	monoclinic
Space group	$P2_1/n$
a/Å	12.339(3)
b/Å	6.4087(16)
c/Å	14.207(3)
α/°	90
β/°	102.801(7)
γ/°	90
Volume/Å^3	1095.5(5)
Z	2
ρ_{calc}g/cm^3	1.802
μ/mm^{-1}	0.142
F(000)	596.0
Crystal size/mm^3	0.12 × 0.12 × 0.1
Radiation	MoKα (λ = 0.71073)
2Θ range for data collection/°	4.952 to 56.708
Index ranges	$-16 \leq h \leq 16$, $-8 \leq k \leq 8$, $-18 \leq l \leq 18$
Reflections collected	14866
Independent reflections	2725 [R_{int} = 0.0605, R_{sigma} = 0.0458]
Data/restraints/parameters	2725/0/203
Goodness-of-fit on F^2	1.058
Final R indexes [I>=2σ (I)]	R_1 = 0.0498, wR_2 = 0.1057
Final R indexes [all data]	R_1 = 0.0839, wR_2 = 0.1220
Largest diff. peak/hole / e Å^{-3}	0.28/-0.31

Table S9: Fractional Atomic Coordinates (×10^4) and Equivalent Isotropic Displacement Parameters (Å^2×10^3) for 8. U_{eq} is defined as 1/3 of of the trace of the orthogonalised U_{IJ} tensor.

Atom	***x***	***y***	***z***	**U(eq)**
O1	1097.3(12)	192(2)	3985.7(12)	28.0(4)
N1	6119.9(14)	8804(3)	3969.9(13)	21.0(4)
N14	1014.1(17)	7153(3)	5743.6(16)	32.5(5)
N2	7048.5(15)	9623(3)	3803.2(14)	23.7(4)
N3	7424.2(15)	8287(3)	3249.3(14)	22.5(4)
N4	6798.3(14)	6602(3)	3024.5(13)	21.2(4)
N13	1689.3(16)	6728(3)	5371.0(14)	25.9(4)
N12	2526.7(15)	6543(3)	4979.9(14)	22.7(4)
N7	4185.8(15)	681(3)	2340.8(14)	23.0(4)
N5	5583.5(14)	2837(3)	2363.9(14)	21.5(4)
N6	5067.2(15)	1034(3)	2012.5(14)	24.2(4)
N8	4110.7(14)	2324(3)	2931.1(13)	18.8(4)
N9	2544.8(14)	1152(3)	3419.3(13)	21.2(4)
N11	1775.7(14)	3261(3)	4505.8(13)	21.0(4)
N10	1812.1(14)	1541(3)	3965.6(13)	21.3(4)

C7	5990.9(17)	6980(3)	3483.5(15)	18.9(4)
C5	4973.7(16)	3654(3)	2933.3(15)	18.6(4)
C6	2535.0(17)	4713(3)	4480.2(16)	19.5(4)
C1	3389.3(16)	4497(3)	3969.7(15)	18.5(4)
C4	5061.9(16)	5558(3)	3471.2(15)	18.7(4)
C3	4254.4(16)	5962(3)	3965.9(15)	19.2(4)
C2	3308.5(16)	2641(3)	3454.4(15)	18.5(4)

Table S10: Anisotropic Displacement Parameters (Å^2×10^3) for 8. The Anisotropic displacement factor exponent takes the form: -2π^2[h^{2}a*^{2}U$_{11}$+2hka*b*U$_{12}$+…].

Atom	U_{11}	U_{22}	U_{33}	U_{23}	U_{13}	U_{12}
O1	22.7(8)	23.8(8)	39.0(10)	-0.6(7)	9.9(7)	-8.0(7)
N1	18.8(8)	18.5(9)	27.4(10)	-1.8(8)	9.0(7)	-2.5(7)
N14	31.4(11)	27.6(11)	44.4(13)	-3.1(10)	20.5(10)	-2.1(9)
N2	21.8(9)	21.6(9)	30.0(11)	1.6(8)	10.8(8)	0.6(8)
N3	21.1(9)	19.1(9)	29.5(11)	-0.7(8)	10.7(8)	-2.0(7)
N4	19.9(9)	18.9(9)	27.4(10)	0.0(8)	10.6(7)	-3.0(7)
N13	25.9(10)	21.1(10)	34.0(11)	-2.1(8)	13.4(9)	-2.7(8)
N12	22.4(9)	19.8(9)	30.5(10)	-2.2(8)	15.6(8)	-0.8(7)
N7	22.4(9)	21.5(9)	26.6(10)	-5.0(8)	8.5(8)	1.1(7)
N5	19.6(8)	20.2(9)	25.7(10)	-1.8(8)	7.1(7)	1.8(7)
N6	21.3(9)	23.6(9)	28.4(11)	-4.6(8)	7.0(8)	-0.2(8)
N8	19.3(8)	16.3(8)	21.9(9)	-3.5(7)	6.8(7)	0.4(7)
N9	19.3(8)	20.7(9)	24.6(10)	-1.0(8)	7.0(7)	-2.1(7)
N11	20.7(9)	18.6(9)	24.4(10)	-0.5(8)	6.6(7)	-0.9(7)
N10	20.0(9)	20.8(9)	24.2(10)	0.0(8)	7.1(7)	-0.5(7)
C7	18.8(9)	18.7(10)	20.1(11)	1.7(9)	6.6(8)	1.6(8)
C5	16.2(9)	18.4(10)	21.9(11)	1.9(9)	5.5(8)	-0.1(8)
C6	18.6(10)	18.7(10)	22.4(11)	2.9(9)	7.2(9)	2.0(8)
C1	18.0(10)	18.3(10)	19.7(11)	1.2(8)	5.3(8)	1.5(8)
C4	17.4(9)	18.1(10)	21.5(11)	1.8(8)	6.1(8)	1.1(8)
C3	19.6(10)	16.6(10)	22.5(11)	0.8(9)	7.1(8)	0.1(8)
C2	17.2(9)	18.2(10)	20.7(11)	2.2(8)	5.5(8)	0.7(8)

Table S11: Bond Lengths for 8.

Atom	Atom	Length/Å	Atom	Atom	Length/Å
O1	N10	1.240(2)	N8	C5	1.363(3)
N1	N2	1.328(2)	N8	C2	1.378(3)
N1	C7	1.350(3)	N9	N10	1.339(2)
N14	N13	1.115(3)	N9	C2	1.335(3)
N2	N3	1.315(3)	N11	N10	1.350(3)
N3	N4	1.325(2)	N11	C6	1.327(3)
N4	C7	1.328(3)	C7	C4	1.462(3)

N13	N12	1.283(2)	C5	C4	1.431(3)
N12	C6	1.372(3)	C6	C1	1.412(3)
N7	N6	1.295(2)	C1	C3	1.423(3)
N7	N8	1.362(2)	C1	C2	1.389(3)
N5	N6	1.360(3)	C4	C3	1.365(3)
N5	C5	1.328(3)			

Table S12: Bond Angles for 8.

Atom	Atom	Atom	Angle/°	Atom	Atom	Atom	Angle/°
N2	N1	C7	105.04(17)	N4	C7	N1	113.14(18)
N3	N2	N1	106.38(17)	N4	C7	C4	123.51(19)
N2	N3	N4	114.26(17)	N5	C5	N8	107.44(18)
N3	N4	C7	101.17(17)	N5	C5	C4	132.46(19)
N14	N13	N12	170.5(2)	N8	C5	C4	120.08(18)
N13	N12	C6	113.72(18)	N12	C6	C1	116.21(19)
N6	N7	N8	105.32(17)	N11	C6	N12	119.93(18)
C5	N5	N6	106.03(17)	N11	C6	C1	123.9(2)
N7	N6	N5	112.23(17)	C6	C1	C3	125.7(2)
N7	N8	C5	108.97(17)	C2	C1	C6	112.35(19)
N7	N8	C2	126.94(17)	C2	C1	C3	121.98(19)
C5	N8	C2	124.09(18)	C5	C4	C7	120.32(18)
C2	N9	N10	114.00(18)	C3	C4	C7	122.35(19)
C6	N11	N10	116.40(17)	C3	C4	C5	117.33(19)
O1	N10	N9	117.27(18)	C4	C3	C1	120.7(2)
O1	N10	N11	116.30(17)	N8	C2	C1	115.75(18)
N9	N10	N11	126.43(17)	N9	C2	N8	117.39(19)
N1	C7	C4	123.34(19)	N9	C2	C1	126.86(19)

Table S13: Torsion Angles for 8.

A	B	C	D	Angle/°	A	B	C	D	Angle/°
N1	N2	N3	N4	0.3(2)	N8	C5	C4	C3	-0.2(3)
N1	C7	C4	C5	179.5(2)	N11	C6	C1	C3	-176.3(2)
N1	C7	C4	C3	-0.8(3)	N11	C6	C1	C2	3.3(3)
N2	N1	C7	N4	0.5(2)	N10	N9	C2	N8	178.27(17)
N2	N1	C7	C4	179.97(19)	N10	N9	C2	C1	-1.4(3)
N2	N3	N4	C7	0.0(2)	N10	N11	C6	N12	177.47(18)
N3	N4	C7	N1	-0.3(2)	N10	N11	C6	C1	-3.4(3)
N3	N4	C7	C4	-179.78(19)	C7	N1	N2	N3	-0.5(2)
N4	C7	C4	C5	-1.0(3)	C7	C4	C3	C1	-177.28(19)
N4	C7	C4	C3	178.6(2)	C5	N5	N6	N7	-0.8(2)
N13	N12	C6	N11	-5.7(3)	C5	N8	C2	N9	-176.68(19)

N13	N12	C6	C1	175.10(19)	C5	N8	C2	C1	3.1(3)
N12	C6	C1	C3	2.8(3)	C5	C4	C3	C1	2.4(3)
N12	C6	C1	C2	-177.55(19)	C6	N11	N10	O1	-179.55(18)
N7	N8	C5	N5	-0.8(2)	C6	N11	N10	N9	0.9(3)
N7	N8	C5	C4	177.56(18)	C6	C1	C3	C4	177.7(2)
N7	N8	C2	N9	3.1(3)	C6	C1	C2	N8	179.56(18)
N7	N8	C2	C1	-177.17(19)	C6	C1	C2	N9	-0.7(3)
N5	C5	C4	C7	-2.7(4)	C3	C1	C2	N8	-0.8(3)
N5	C5	C4	C3	177.7(2)	C3	C1	C2	N9	178.9(2)
N6	N7	N8	C5	0.3(2)	C2	N8	C5	N5	179.00(18)
N6	N7	N8	C2	-179.49(19)	C2	N8	C5	C4	-2.6(3)
N6	N5	C5	N8	0.9(2)	C2	N9	N10	O1	-178.13(18)
N6	N5	C5	C4	-177.1(2)	C2	N9	N10	N11	1.4(3)
N8	N7	N6	N5	0.3(2)	C2	C1	C3	C4	-1.9(3)
N8	C5	C4	C7	179.43(19)					

Table S14: Hydrogen Atom Coordinates (Å×10^4) and Isotropic Displacement Parameters (Å^2×10^3) for 8.

Atom	*x*	*y*	*z*	U(eq)
H3A	4270.43	7235.66	4311.13	23
H3	8140(20)	8510(50)	3000(20)	56(9)

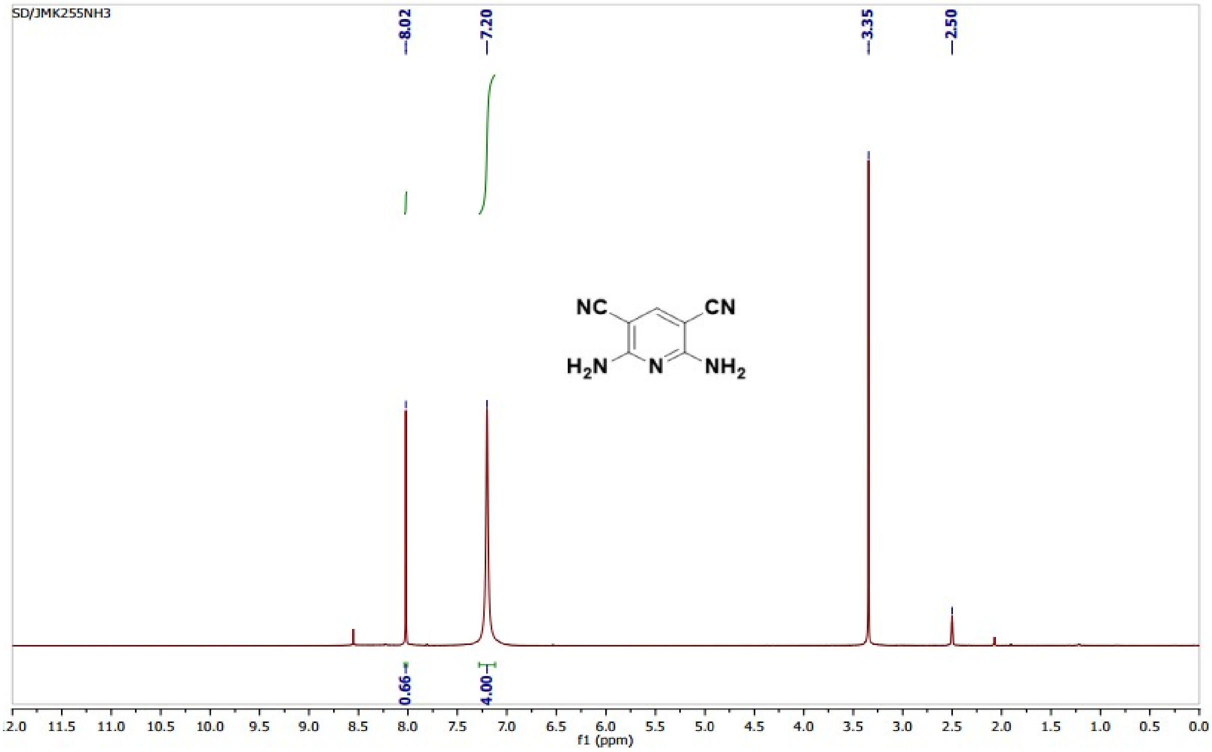

Figure S3: ^{1}H NMR spectrum of Compound **3** (recorded in DMSO-d$_6$; 400 MHz).

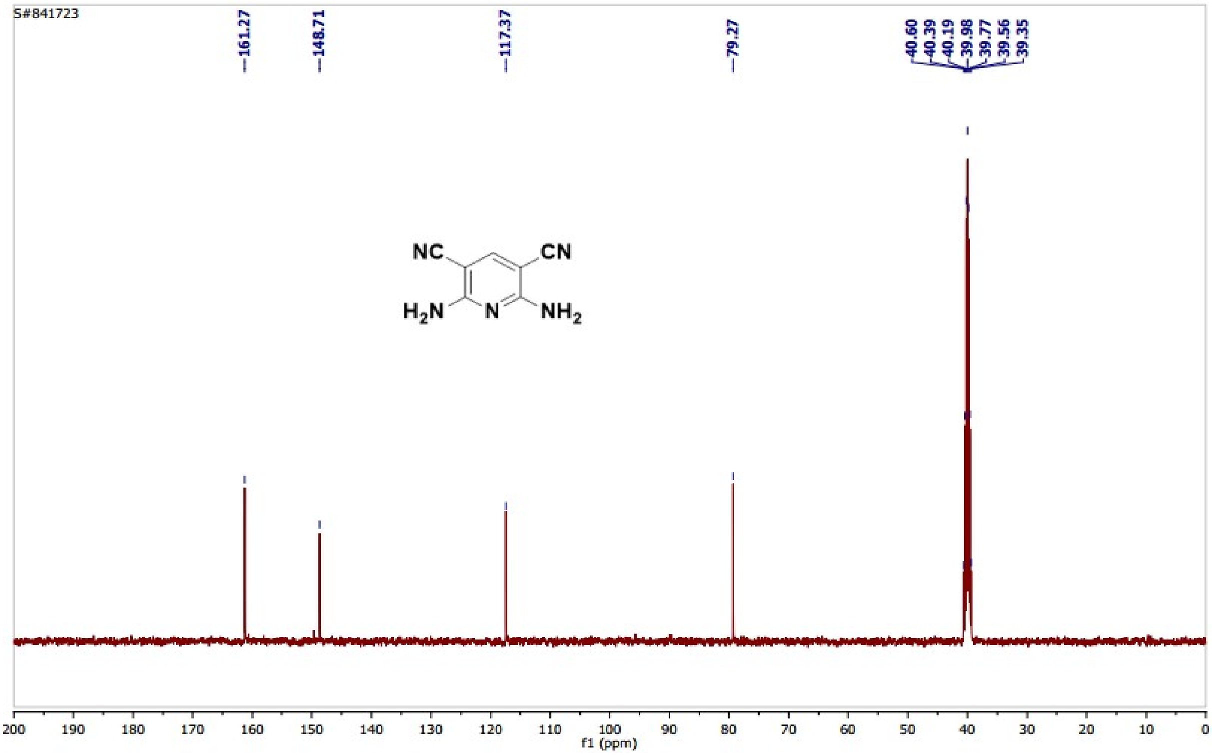

Figure S4: ^{13}C{^{1}H} NMR spectrum of compound **3** (recorded in DMSO-d$_6$; 100 MHz).

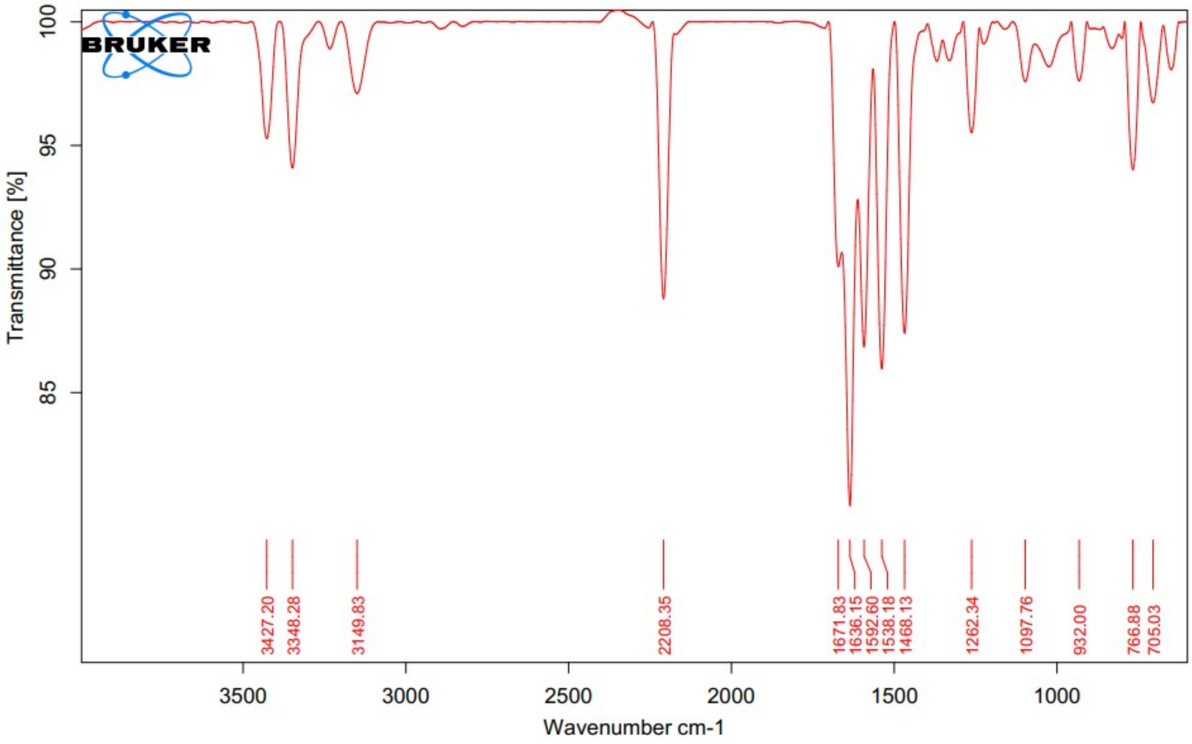

Figure S5: IR spectrum of compound **3.**

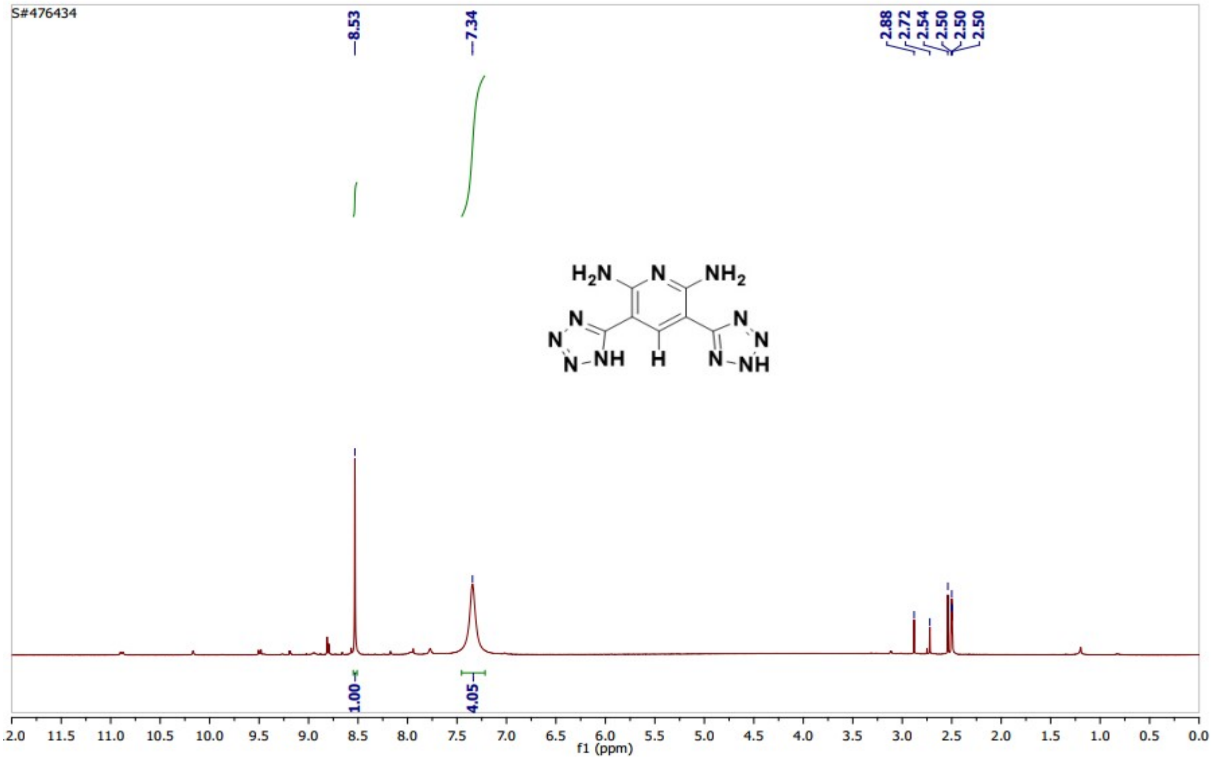

Figure S6: ^{1}H NMR spectrum of Compound **4** (recorded in DMSO-d_6; 400 MHz).

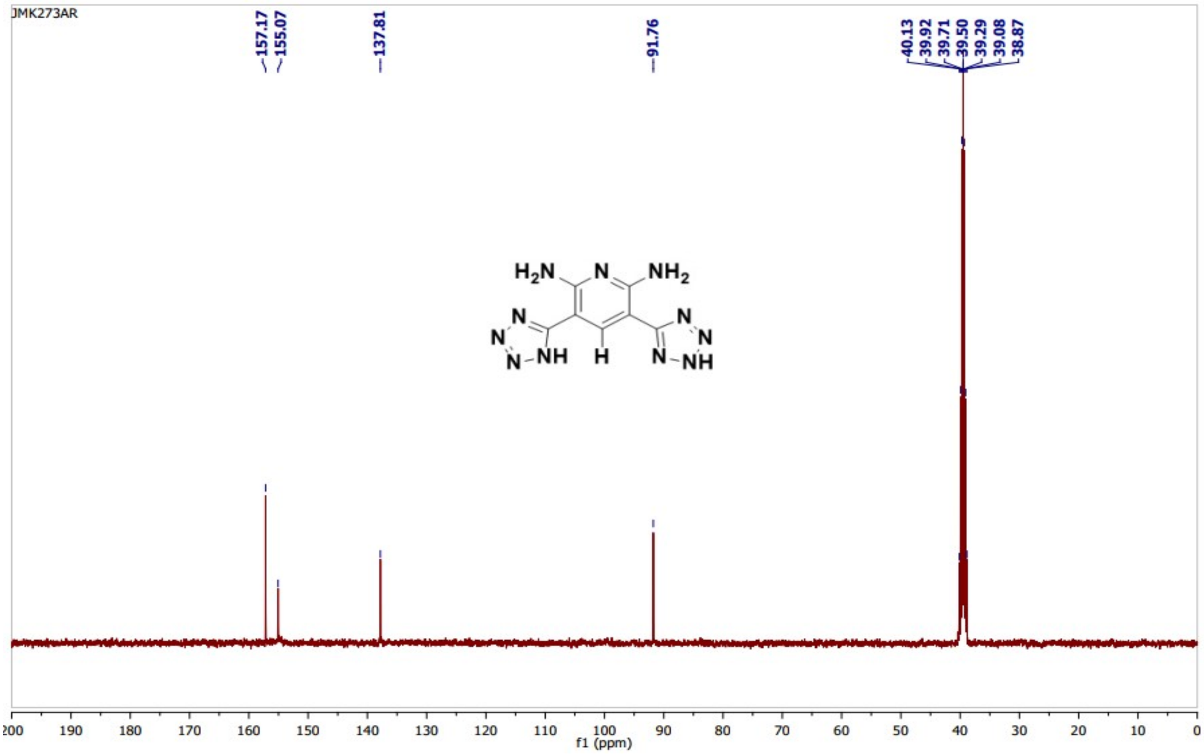

Figure S7: $^{13}C\{^{1}H\}$ NMR spectrum of compound **4** (recorded in DMSO-d_6; 100 MHz).

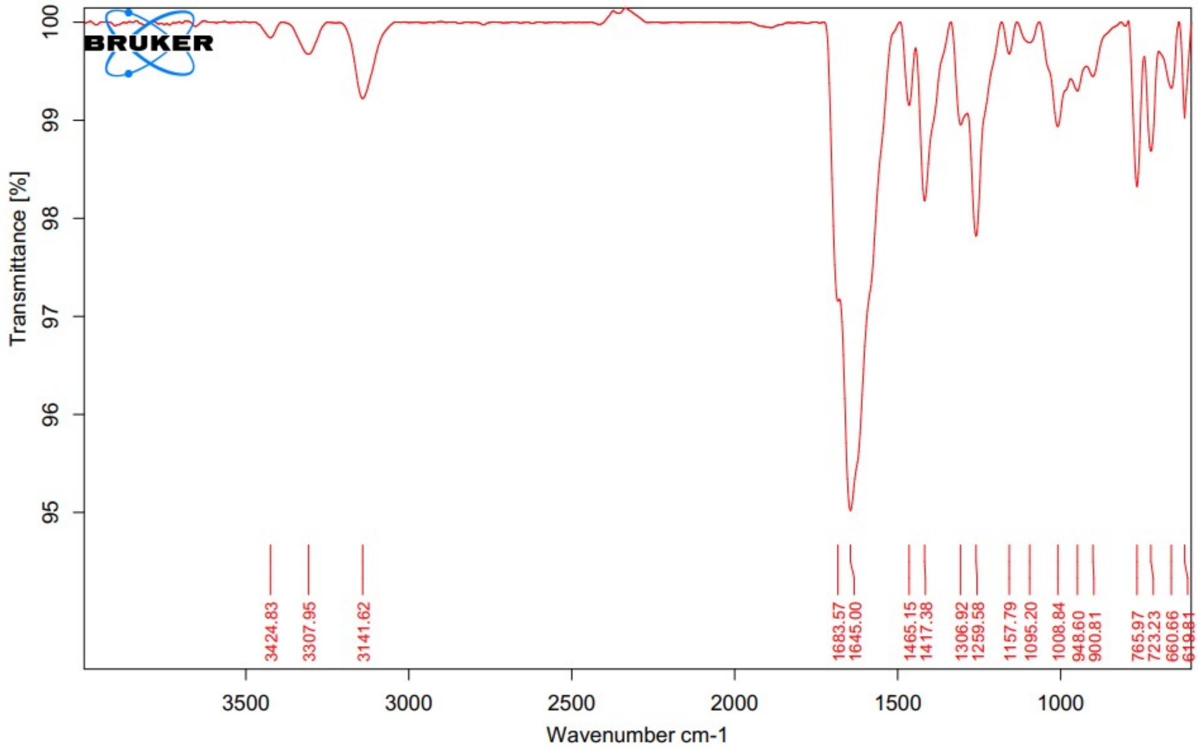

Figure S8: IR spectrum of compound **4.**

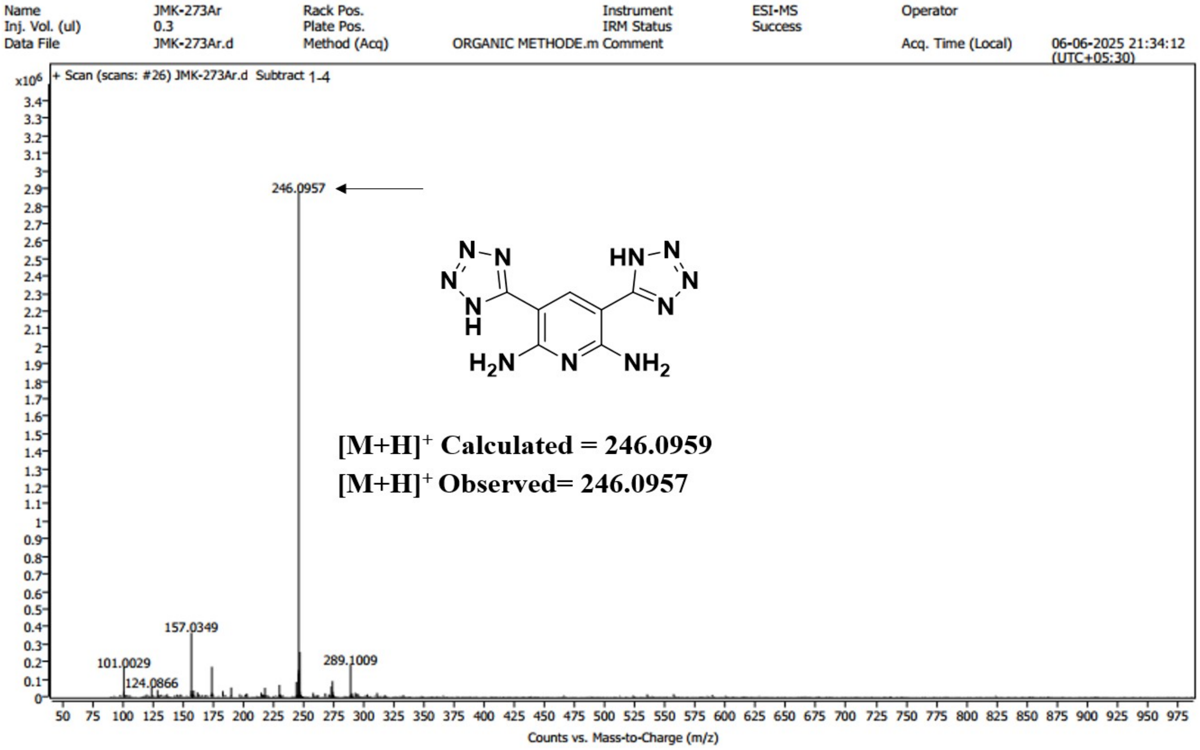

Name	JMK-273Ar	Rack Pos.	Instrument	ESI-MS	Operator
Inj. Vol. (ul)	0.3	Plate Pos.	IRM Status	Success	
Data File	JMK-273Ar.d	Method (Acq) ORGANIC METHODE.m	Comment		Acq. Time (Local) 06-06-2025 21:34:12 (UTC+05:30)

$[M+H]^+$ Calculated = 246.0959

$[M+H]^+$ Observed= 246.0957

Figure S9: Mass spectrum of compound **4.**

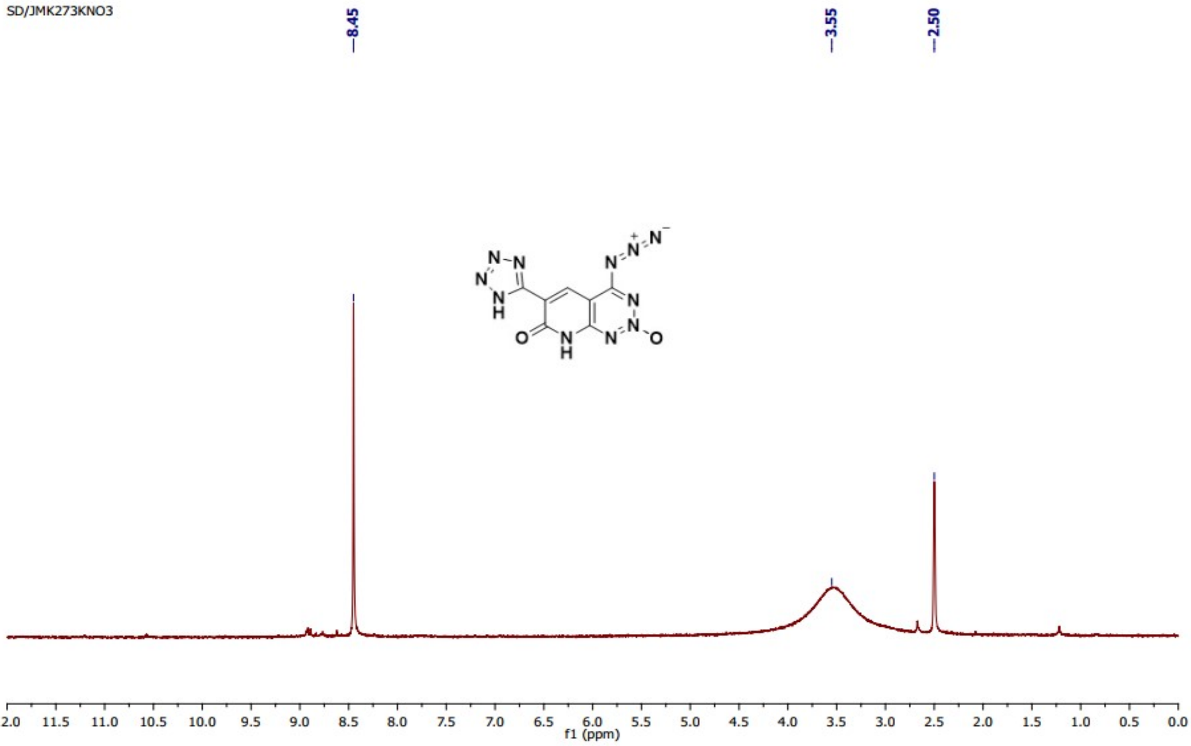

Figure S10: ^{1}H NMR spectrum of Compound **5** (recorded in DMSO-d_6; 400 MHz).

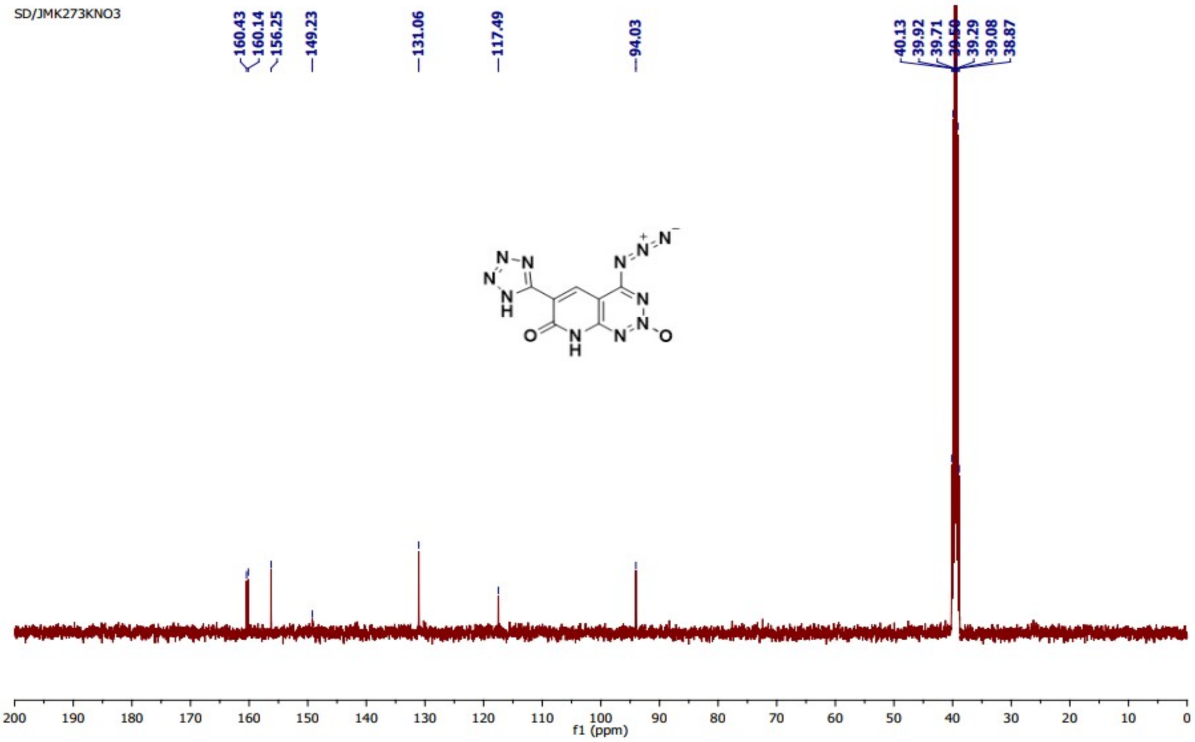

Figure S11: $^{13}C\{^1H\}$ NMR spectrum of compound **5** (recorded in DMSO-d_6; 100 MHz).

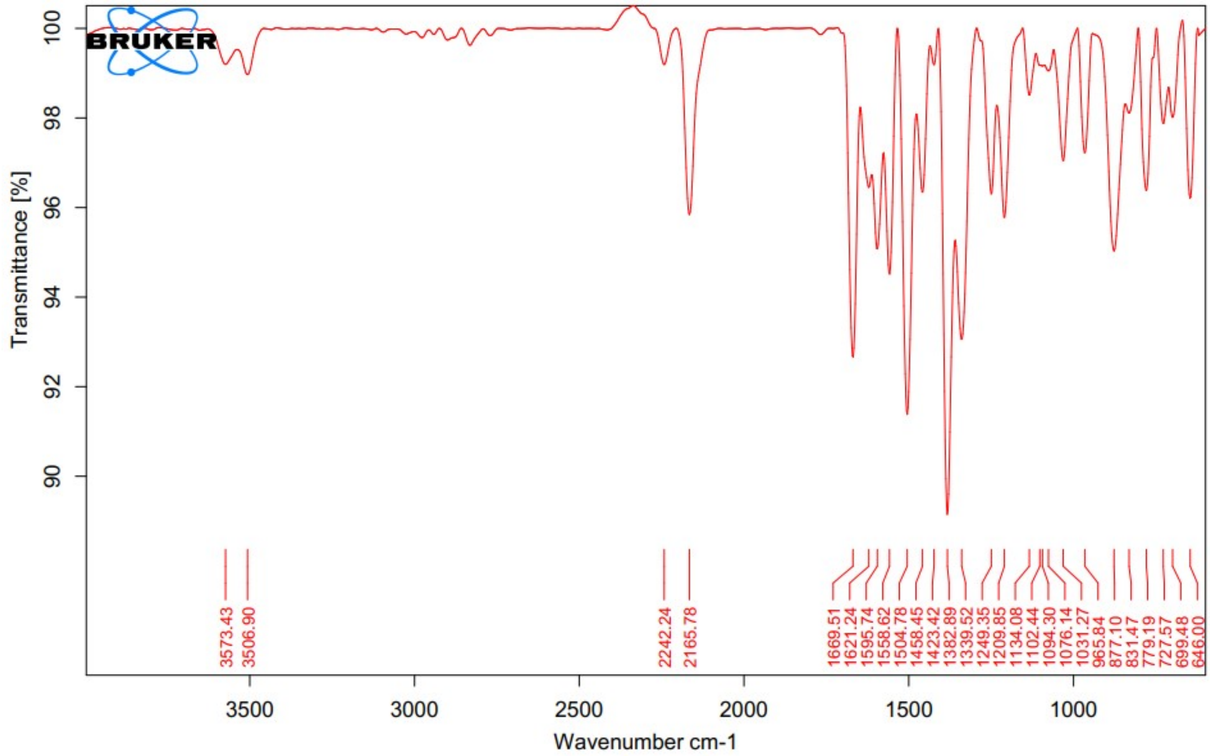

Figure S12: IR spectrum of compound **5.**

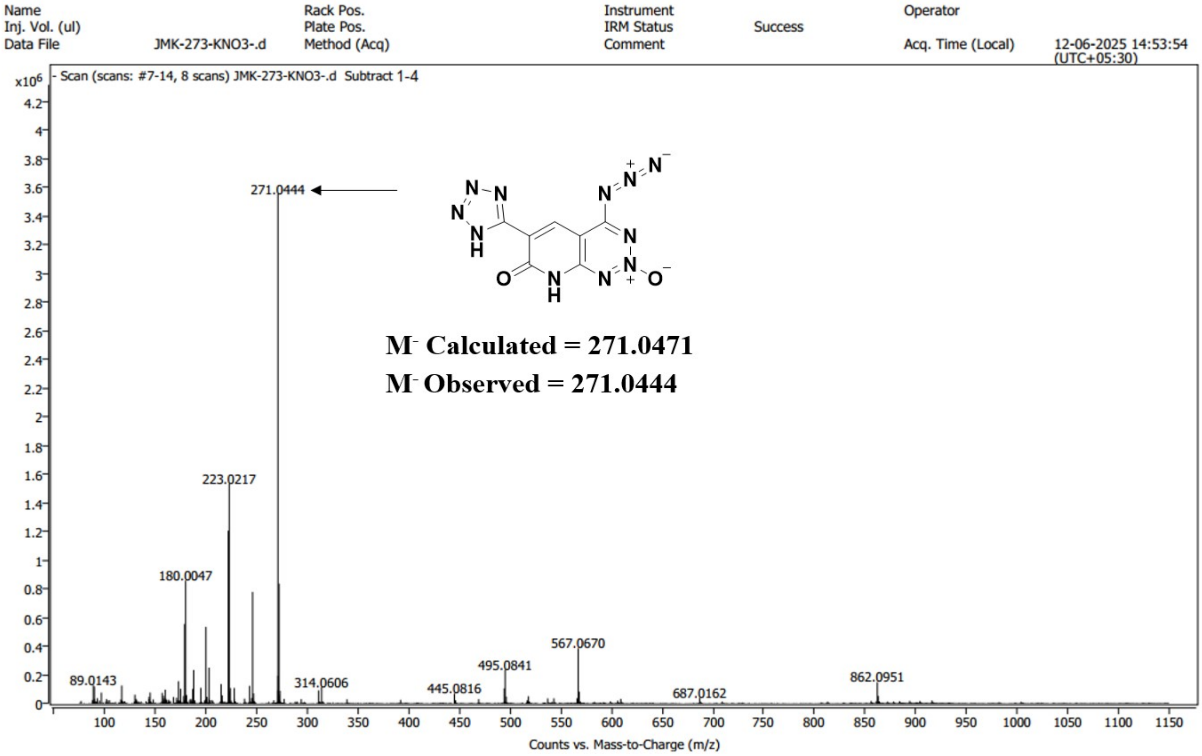

M^- Calculated = 271.0471

M^- Observed = 271.0444

Figure S13: Mass spectrum of compound **5.**

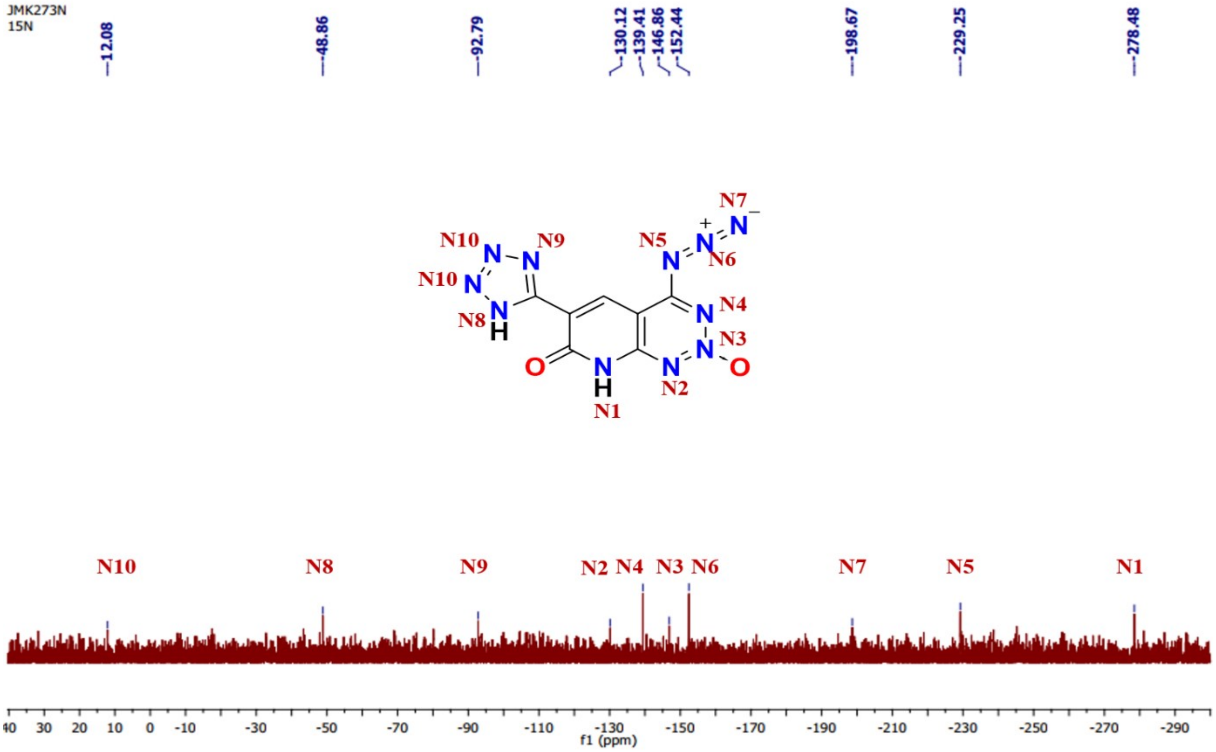

Figure S14: ^{15}N NMR of compound **5.**

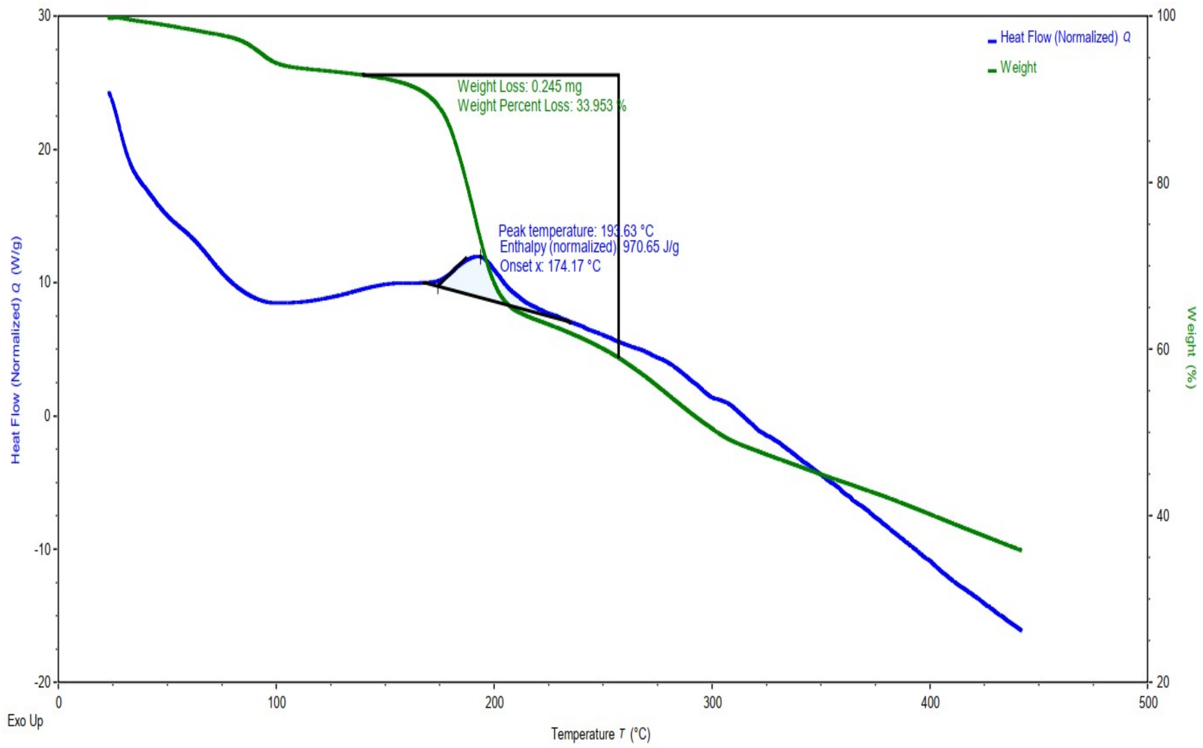

Figure S15: TGA-DSC of compound **5.**

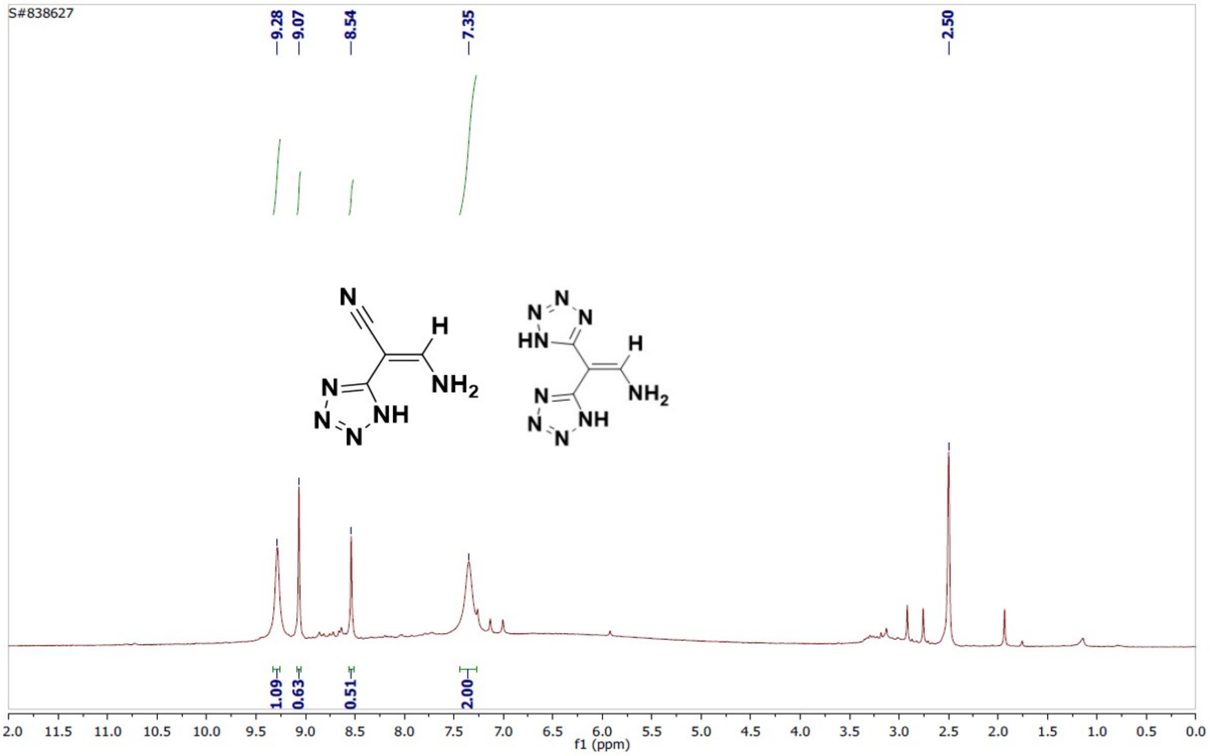

Figure S16: ^{1}H NMR spectrum of Compound **7M** (recorded in DMSO-d$_6$; 400 MHz).

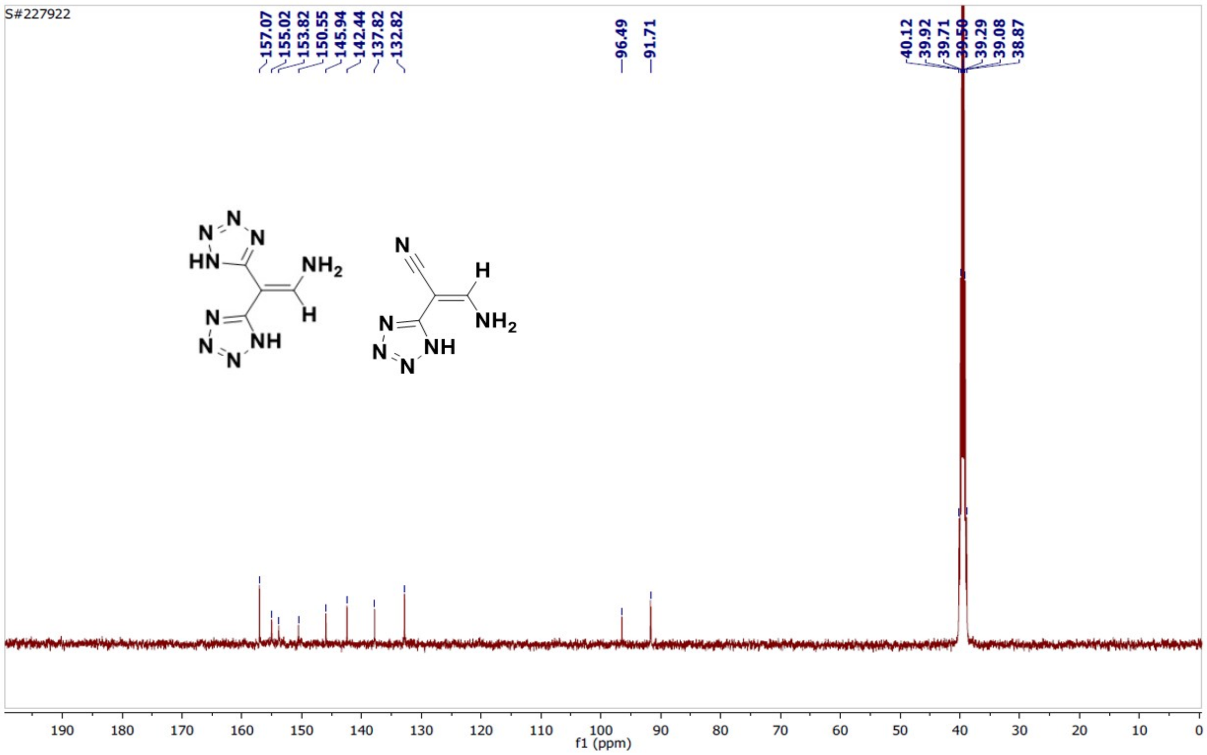

Figure S17: $^{13}C\{^1H\}$ NMR spectrum of compound **7M** (recorded in DMSO-d$_6$; 100 MHz).

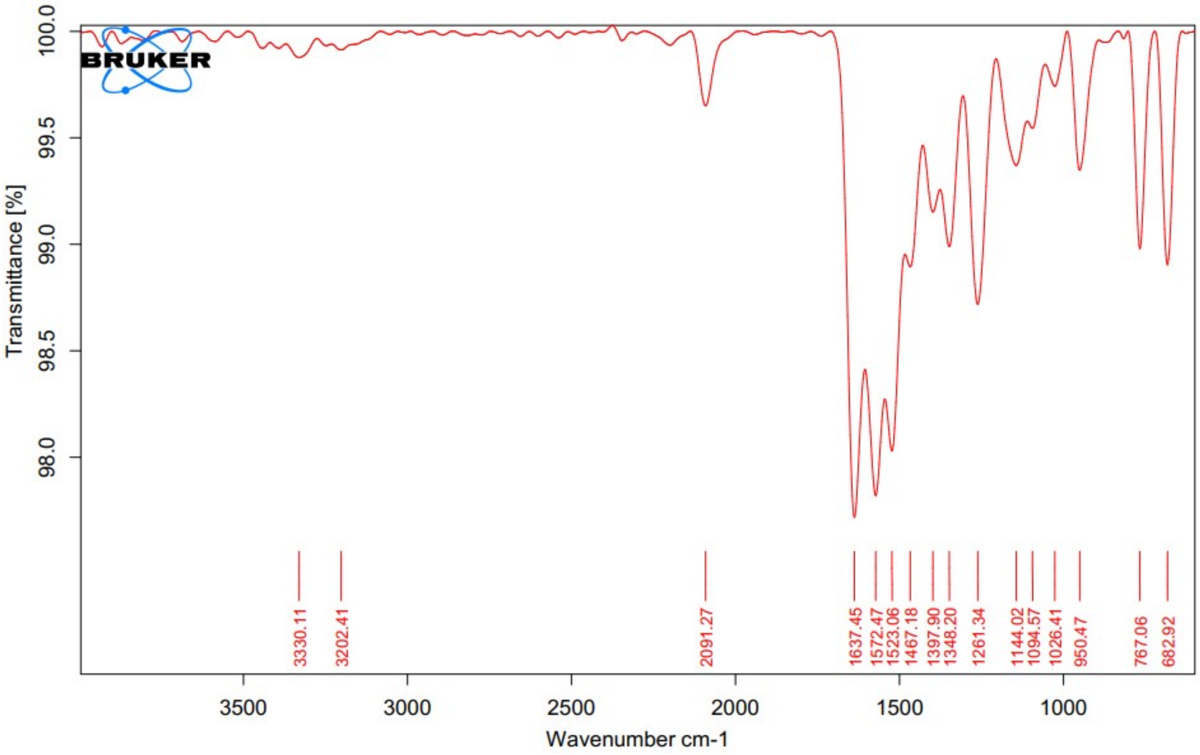

Figure S18: IR spectrum of compound **7M.**

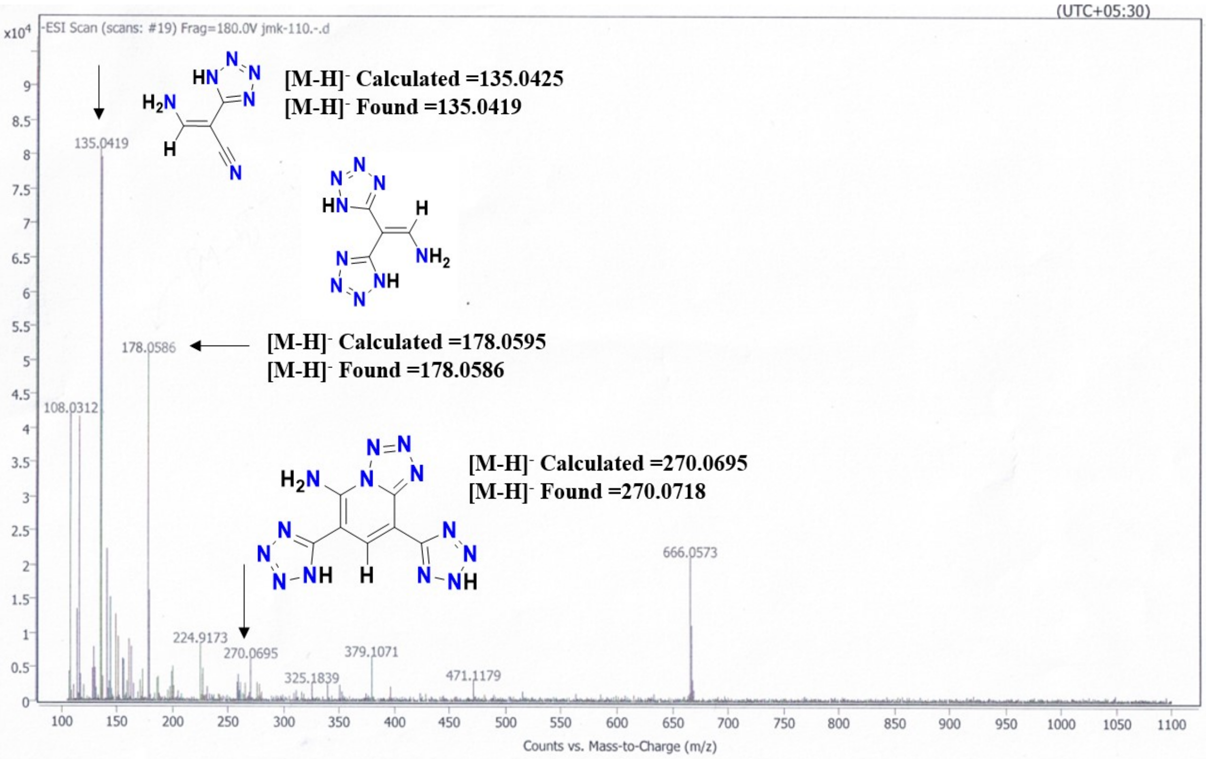

Figure S19: Mass spectrum of Compound **7M.**

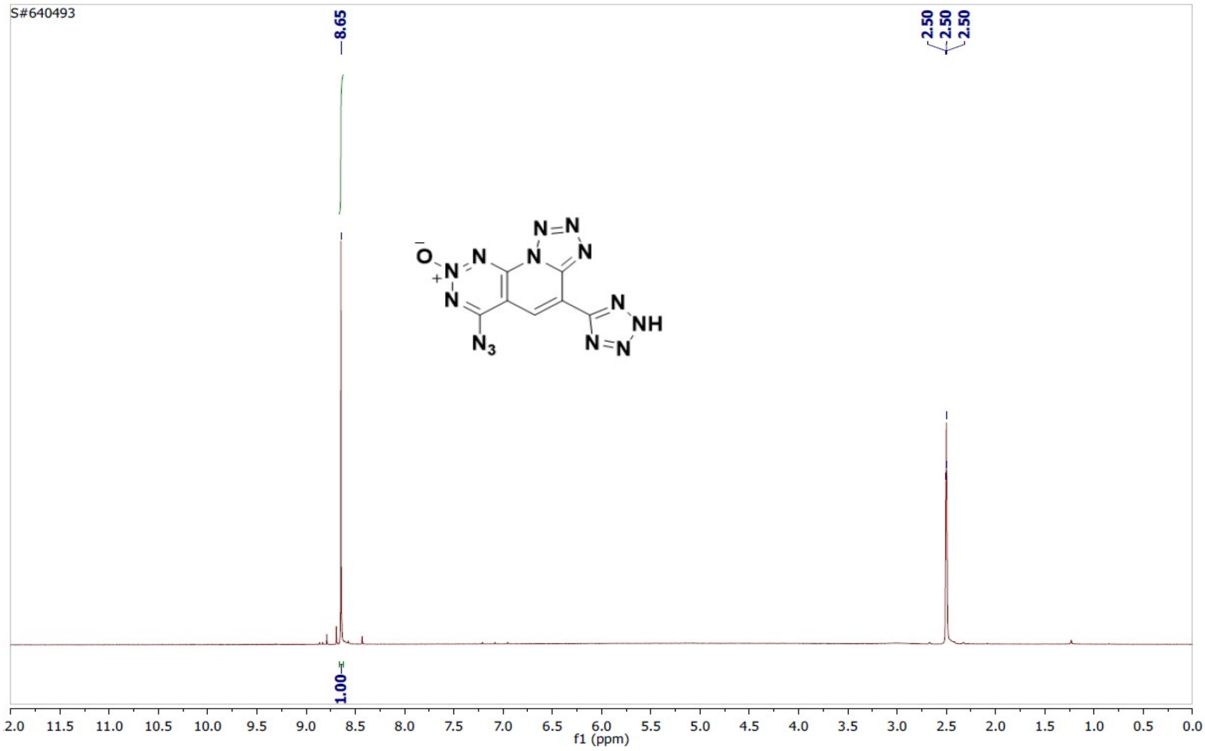

Figure S20: ^{1}H NMR spectrum of Compound **8** (recorded in DMSO-d_6; 400 MHz).

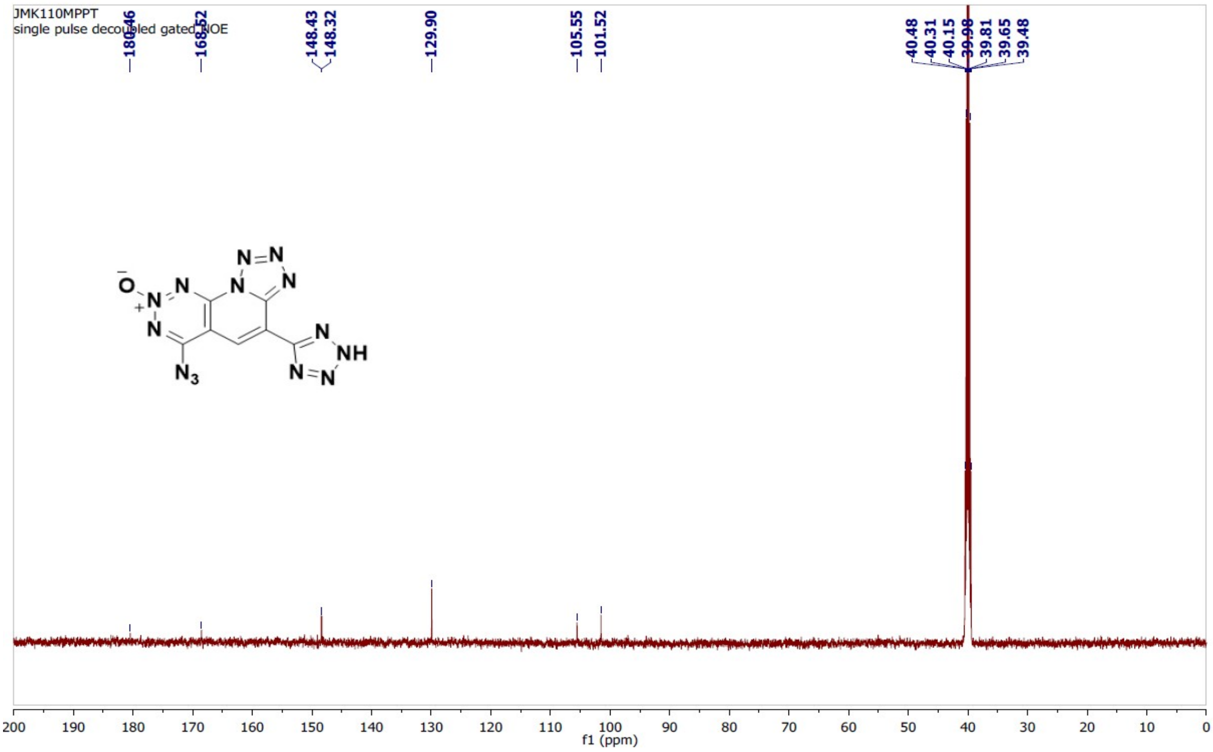

Figure S21: $^{13}C\{^{1}H\}$ NMR spectrum of compound **8** (recorded in DMSO-d_6; 100 MHz).

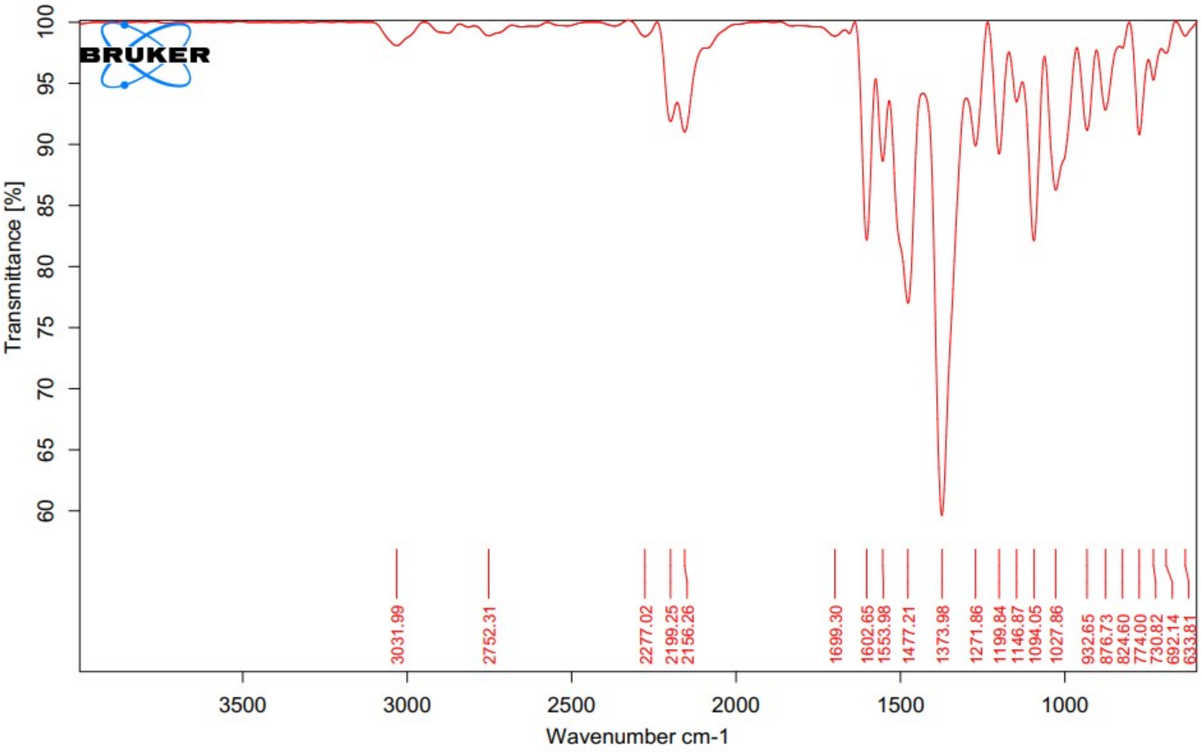

Figure S22: IR spectrum of compound **8.**

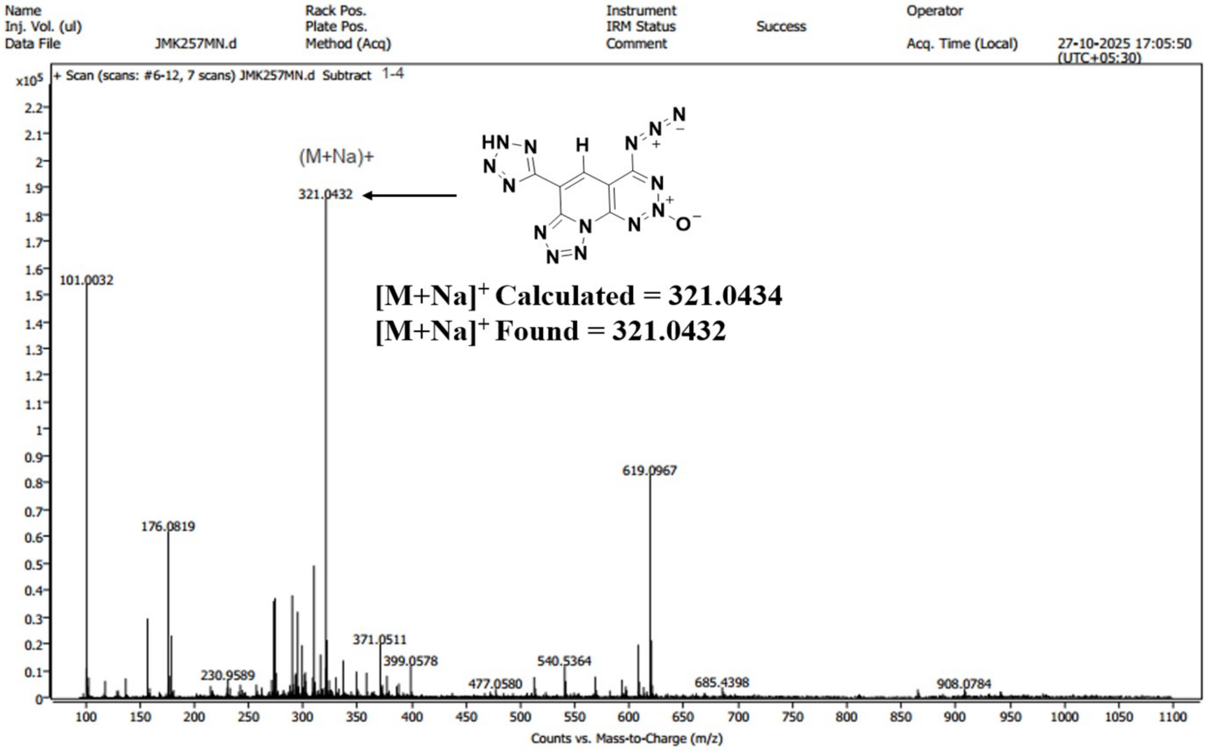

Figure S23: Mass spectrum of compound **8.**

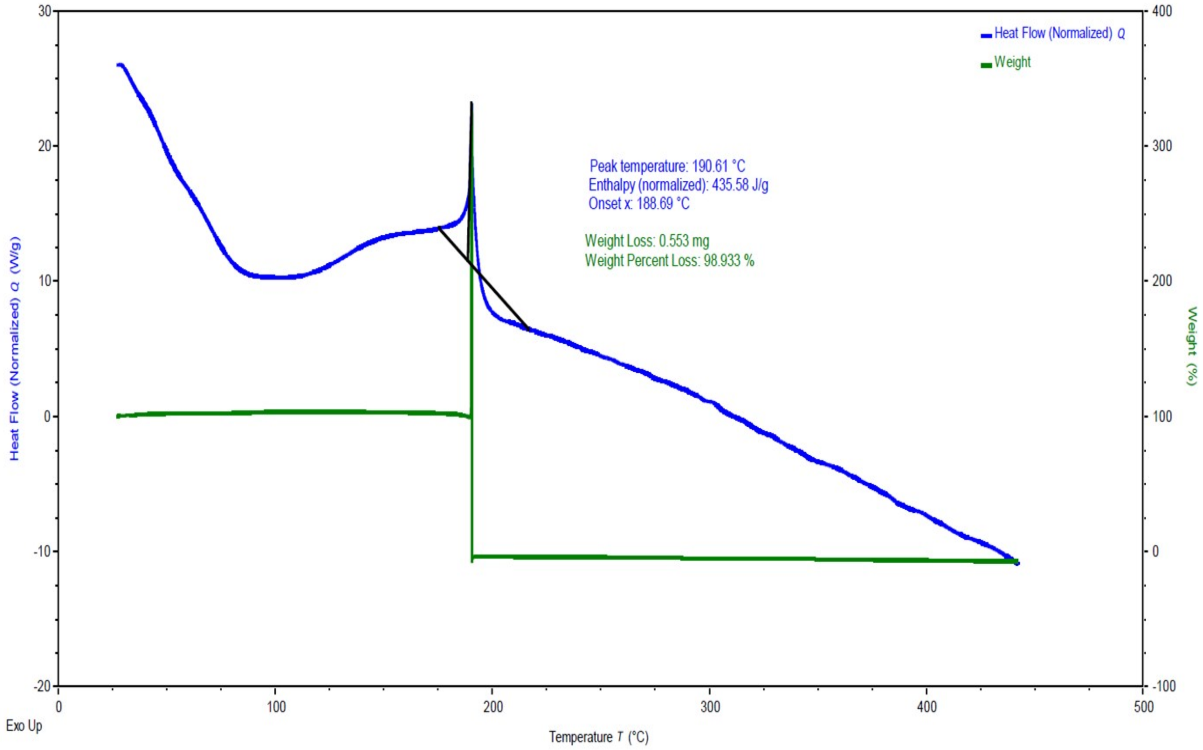

Figure S24: Mass spectrum of compound **8.**

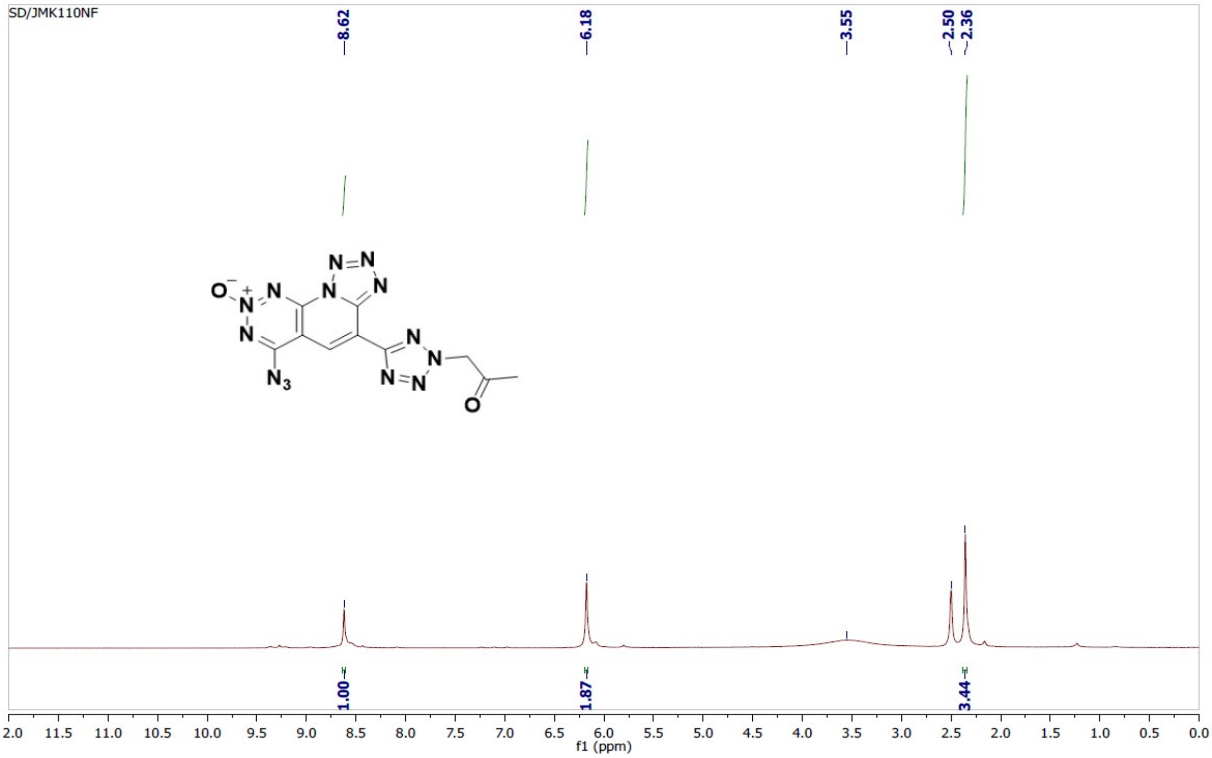

Figure S25: ^{1}H NMR spectrum of Compound **9I** (recorded in DMSO-d$_6$; 400 MHz).

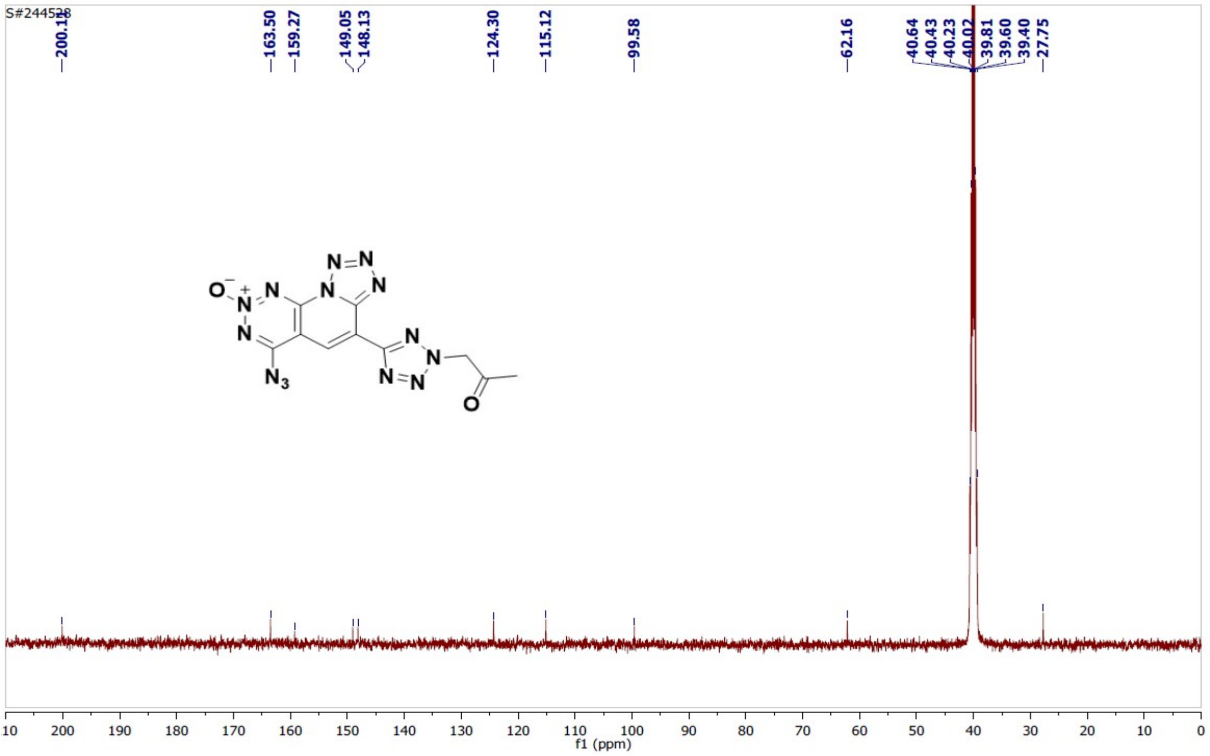

Figure S26: ^{13}C{^{1}H} NMR spectrum of compound **9I** (recorded in DMSO-d$_6$; 100 MHz).

^{15}N NMR Spectrum:

The ^{15}N NMR spectrum of compound **5** was obtained in DMSO-d_6, and the chemical shifts were externally referenced to nitromethane (CH_3NO_2) (**Figure S27**). Signal assignments for the chemically distinct nitrogen atoms were made by comparison with relevant literature data.[6-9] As anticipated from the molecular structure, compound **5** contains ten non-equivalent nitrogen atoms, each giving rise to a separate resonance. The nitrogen atoms of the tetrazole ring exhibited resonances at δ = 12.08 ppm (N10) and at δ = -48.46 ppm (N8) and -92.97 ppm (N9). Nitrogen atoms in the 1,2,3-triazine ring adjacent to the N-oxide moiety appeared at δ = -130.12 ppm (N2) and -139.41 ppm (N4), while the N-oxide-bearing nitrogen (N3) resonated at δ = -146.86 ppm. The azide functional group displayed three characteristic peaks at δ = -152.44 ppm (N6), -198.67 ppm (N7), and -229.25 ppm. The pyridine nitrogen gave the most downfield signal at δ = -278.48 ppm (N1). These results unequivocally confirm the presence of ten distinct nitrogen environments within the molecular framework of compound **5**.

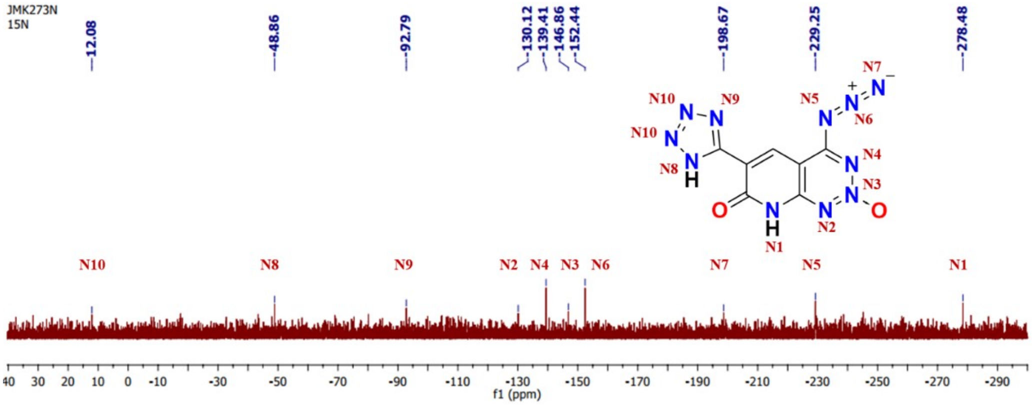

Figure S27: ^{15}N NMR spectrum of Compound **5**.

Mechanism:

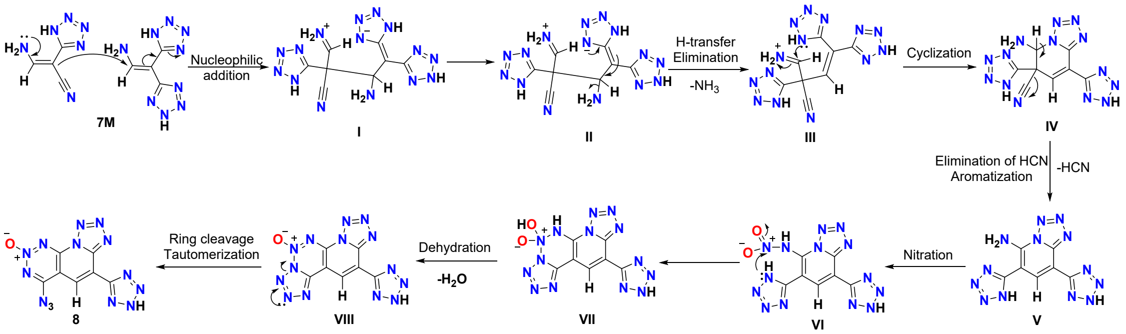

Scheme S1: Proposed mechanism for the synthesis of compound **8**.

The synthesis of compound **8** can be rationalized by a proposed acid-catalysed intermolecular rearrangement mechanism of **7M** as shown in **Scheme S1**. In this mechanism, as shown in **7M**, the lone pair of the amine group in the mono cyclized product makes a nucleophilic attack on the carbon centre of the bicyclic product, generating intermediate **I** and subsequent release of NH_3 affords intermediate **III** which undergoes intramolecular cyclization (intermediate **IV**) followed by elimination of hydrogen cyanide (HCN) to give a stable intermediate **V**, as confirmed by HRMS. Intermediate **V** is further proposed to undergo nitramino formation, intramolecular cyclization, and dehydration to yield intermediate **VII**, which, after tetrazole ring cleavage, furnishes compound **8**.

Hirshfeld surface:

To further visualize the intermolecular interactions in the crystal structures of compounds **5** and **8**, Hirshfeld surface and two-dimensional fingerprint analyses were employed. Red spots on the Hirshfeld surface indicate strong interactions between atoms where their distance is shorter than the van der Waals distance, whereas blue and white spots indicate weaker interactions. The Hirshfeld surfaces of **5** and **8** are shown in **Figures S28a** and **S28d**, offering planar configurations. The strong intermolecular hydrogen-bonding interactions, particularly H···O/O···H and H···N/N···H contacts, are primarily responsible for the prominent red spots observed on the surfaces. These interactions are essential for maintaining the stability of the crystal packing. **Figures S28b** and **S28e** show that the 2D fingerprint plots of compounds **5** and **8** have two distinct spikes attributable to hydrogen-bonding (HB) interactions. The percentage contributions of HBs (N···H and O···H) for **5** and **8** were 44.9% and 21.5%, respectively, indicating that hydrogen bonding stabilizes these energetic compounds and improves thermal stability and insensitivity, as illustrated in **Figures S28c** and **S28f**. Comparatively, compound **5** has 18% N···N and 7.1% O···N interactions, which are responsible for its lower sensitivity, whereas compound **8**, with 39.2% N···N and 15.1% O···N, is accountable for its sensitivity to impact and friction. The coplanar structures of compounds **5** and **8** allow for a layer-by-layer molecular arrangement within their crystal lattices, making it more feasible to develop π-π stacking interactions. Non-covalent interactions such as C···N and C···O contacts were consistent across the crystal structures, with average contributions of 12.9% and 17.6%, respectively.

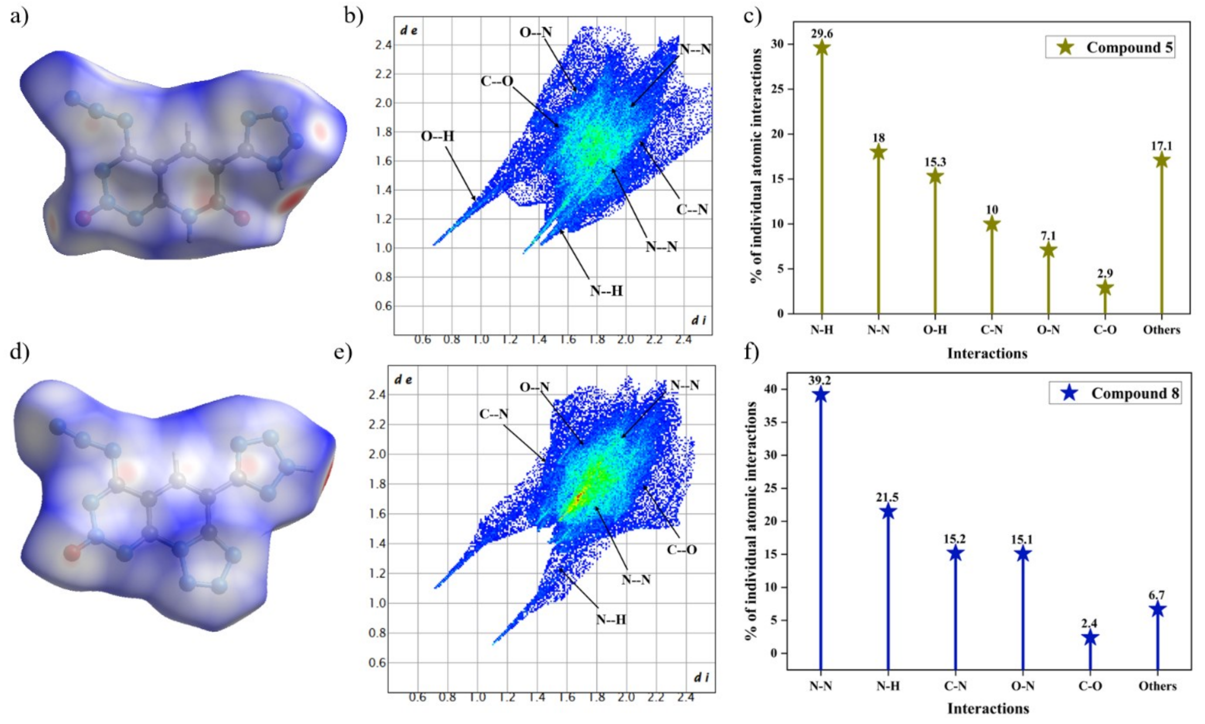

Figure S28: (a-c) Hirshfeld surface, 2D-fingerprint plots, and corresponding individual atomic interactions of compound **5**. (d-f) Hirshfeld surface, 2D-fingerprint plots, and corresponding individual atomic interactions of compound **8.**

Electrostatic potential

Electrostatic potential (ESP) quantitatively describes the variation in charge distribution within a molecule, characterized by positive and negative potential regions in the surrounding space.[10,11] Earlier studies demonstrated a clear correlation between the impact sensitivity of EMs and their ESP, where energetic molecules with higher positive ESP regions over trigger linkages such as C–NO_2, N-NO_2, O-NO_2 and N–N bonds, are found to be associated with increased impact sensitivity and low thermal stability as these bonds are more prone to break under mechanical stimulus.[12, 13] The molecular ESP maps for compounds **5** and **8** were computed on the 0.001 au contour of the electronic density and are shown in **Figure. S29**. The ESP surface local minima (blue region) signify areas of high electron density, while maxima (red region) indicate areas of low electron density. From **Figure S29**, it can be observed that the high electron density regions mainly localized on the catenated nitrogens and N-oxide in compounds **5** and **8**, and these sites are potential contributors to intermolecular interactions and crystal packing. Whereas low electron density regions are mainly associated with carbon and hydrogen atoms. The ESP minima and maxima in compound **5** are -37.71 and 57.70 kcal/mol, while those of compound **8** are -44.71 and 70.53 kcal/mol, respectively. Compound **5** shows better charge distribution in the molecular ESP contour compared to compound **8**, which tends to have higher insensitivity to impact and friction stimuli.

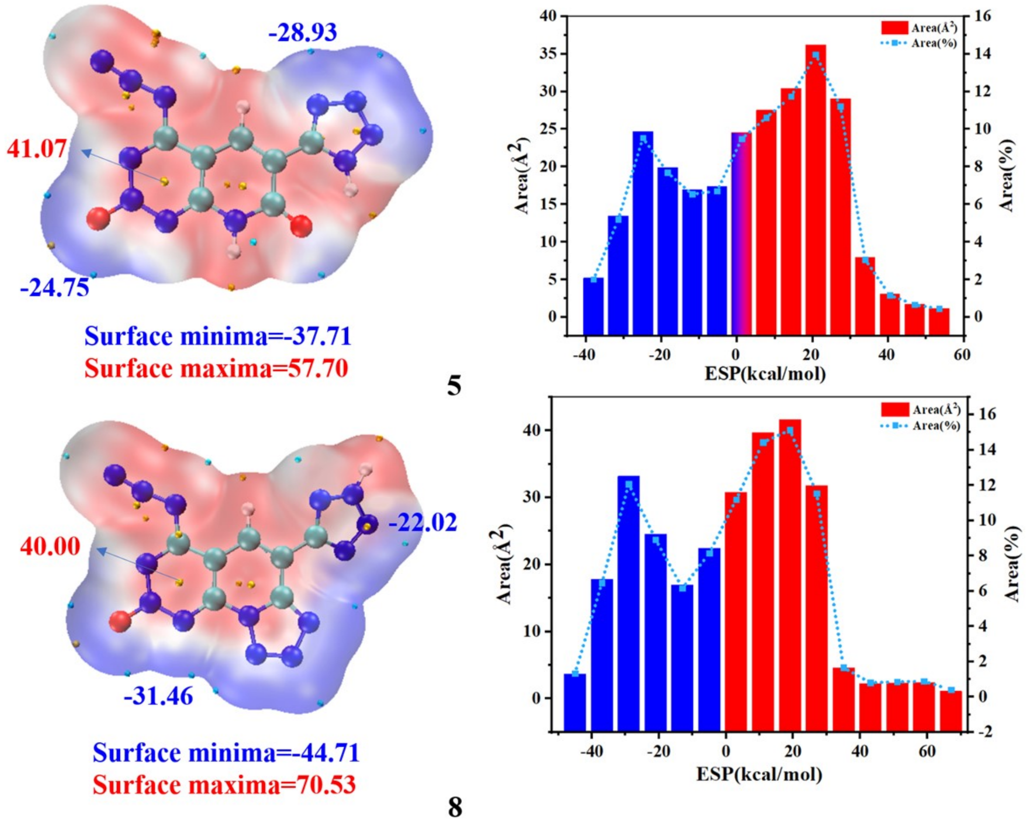

5

8

Figure S29. ESP maps of compounds **5** and **8** with the distribution of surface potentials.

Hot needle test:

To further understand its energetic behaviour, the deflagration-to-detonation transition (DDT) of compound **8** was closely monitored. A hot needle test, which evaluates sensitivity under limited confinement, was conducted by placing a small sample on a metal plate and touching it with a red-hot needle. In this test, compound **8** exhibited DDT behaviour, as shown in **Figure S30**. This strong DDT response is attributed to the preferential cleavage of C-N and N-N bonds, facilitated by the presence of tetrazole rings and azide groups (C-N_3 bonds) within the 1,2,3-triazine ring. These findings indicate that compound **8** possesses the ability to initiate detonation. Furthermore, its stability at room temperature suggests that it could serve as a promising substitute for existing industrial standards.

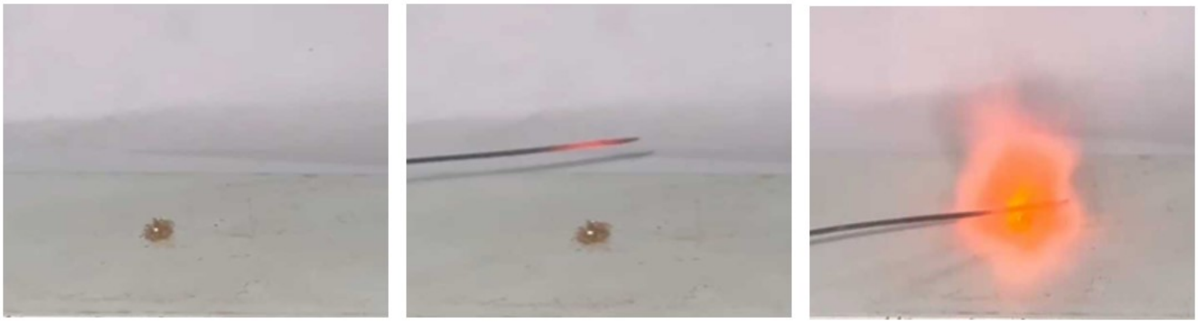

Figure S30: Snapshots of the hot needle test of compound **8**.

Computational details:

Computations were carried out using the Gaussian 09 program suite.[1] The structure optimizations are performed with B3LYP/6-31+G(d,p) level of theory and characterized to be true local energy minima on the potential energy surface, and no imaginary frequencies were found. Heat of formation (HOF) is a measure of the energy content of an energetic material that can decompose, ignite, and explode by heat or impact. It enters into the calculation of explosive and propellant properties such as detonation velocity, detonation pressure, heat of detonation and specific impulse. However, it is impractical to determine the HOF of novel energetic materials because of their unstable intermediates and unknown combustion mechanisms. Gas-phase heats of formation for neutral compounds and anions were calculated using the designed isodesmic reactions (see **Figure S31**). Calculated total energies and related data for reference compounds and target compounds are listed in **Tables S15** and **S16**. The usage of the HOF_{Gas} in the calculation of detonation properties slightly overestimates the values of detonation velocity and detonation pressure, and hence, the solid phase HOF (HOF_{Solid}) has been calculated, which can efficiently reduce the errors. The HOF_{Solid} is calculated as the difference between HOF_{Gas} and heat of sublimation (HOF_{Sub}) as,

$$HOF_{Solid} = HOF_{Gas} - HOF_{Sub} \tag{1}$$

The heat of sublimation (HOF_{Sub}), which is required to convert the HOF_{Gas} to the HOF_{Solid}, was calculated from Equation (2),[2]

$$HOF_{Sub} = 0.000267\,A^2 + 1.650087\,\left(\nu\sigma_{tot}^2\right)^{0.5} - 2.966078 \qquad (2)$$

Where A represents the surface area of the 0.001 electrons/bohr^3 isosurface of electronic density, ν denotes the degree of balance between the positive and negative surface potentials, and σ_{tot}^2 is the electrostatic potential variance. These molecular surface properties were obtained using the Multiwfn program[3] and listed in **Table S17**.

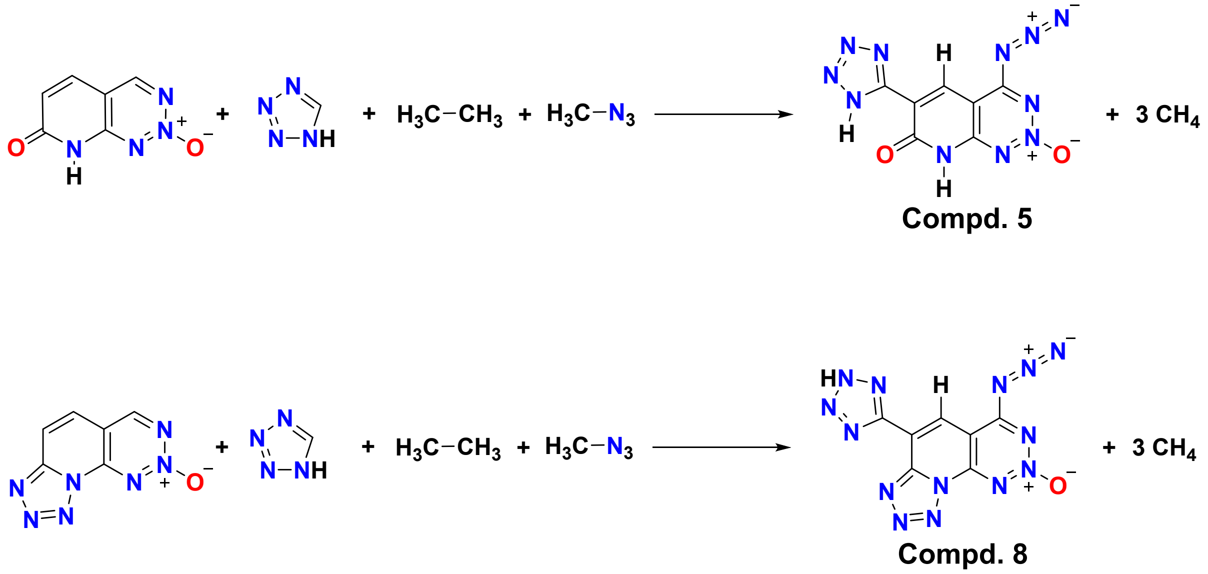

Figure S31. Designed isodesmic reactions to compute gas-phase heats of formation for neutral compounds and anionic components.

Table S15. Calculated total energies at 298K (E_0), zero-point energies (ZPE), and thermal corrections (H_T), and experimental HOFgas of reference compounds used in isodesmic reactions.

Compd.	E_0 (a.u.)	ZPE (au)	H_T (au)	HOF_{gas} (kJ/mol)
CH_4	-40.477548	0.0447	0.0038	-74.8
H_3C-CH_3	-79.762612	0.0746	0.0044	-84
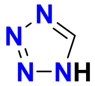	-258.220573	0.0475	0.0044	322.9
H_3C-N_3	-204.049785	0.0502	0.0054	298

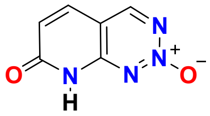	-600.324746	0.1084	0.0093	251.56^a
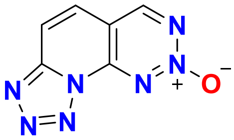	-688.66958	0.1077	0.01	770.9^a

^{a}Calculated using G2 method.

Table S16. Calculated total energies (E_0), zero-point energies (ZPE), and thermal corrections (H_T) for target compounds and their anions.

Compd.	**E_0 (a.u.)**	**ZPE (au)**	**H_T (au)**	**HOF$_{gas}$ (kJ/mol)**	**HOF$_{Sub}$ (kJ/mol)**
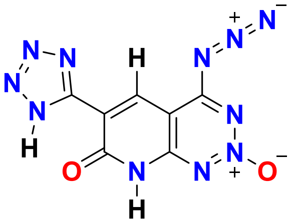	-1020.969701	0.1391	0.0155	882.8	136.7
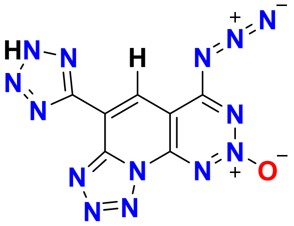	-1109.302892	0.1384	0.0164	1445.6	151.9

Table S17. Calculated molecular surface properties for neutral compounds.

Compd.	**Surface area (Å^2)**	**Volume (Å^3)**	**σ_{tot}^2 (kcal/mol)**	**ν**
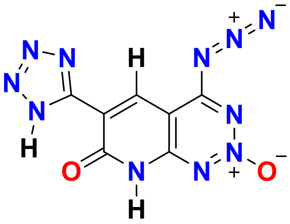	259.11	269.57	211.57	0.2404

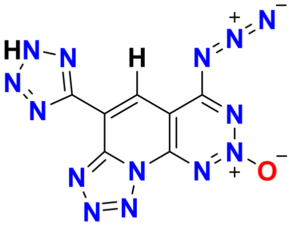	275.07	289.64	267.32	0.2370

Table S18. Optimized coordinates of compd. **5** at B3LYP/6-31+G(d,p) level of theory.

6	-0.825883000	0.011380000	-0.000112000
6	-0.935970000	-1.392416000	-0.000056000
6	0.460998000	0.616707000	-0.000089000
7	0.206873000	-2.136576000	0.000015000
6	1.595535000	-0.152529000	-0.000028000
6	1.505697000	-1.619254000	0.000013000
6	-2.078437000	0.662949000	-0.000084000
7	-3.243646000	0.019949000	-0.000144000
7	-2.088302000	-2.073660000	-0.000105000
7	-3.208163000	-1.337196000	-0.000504000
6	2.916704000	0.459521000	0.000009000
7	4.098523000	-0.194597000	0.000067000
7	3.178077000	1.762421000	-0.000008000
7	5.096010000	0.708073000	0.000088000
7	4.526991000	1.875391000	0.000048000
7	-2.087569000	2.050472000	-0.000003000
7	-3.216993000	2.600266000	0.000031000
7	-4.145748000	3.243089000	0.000019000
8	2.468047000	-2.386669000	0.000077000
8	-4.288444000	-1.924951000	0.000611000

1	0.547714000	1.698408000	-0.000102000
1	0.122656000	-3.149084000	0.000057000
1	4.248554000	-1.197947000	0.000083000

Table S19. Optimized coordinates of compd. 8 at B3LYP/6-31+G(d,p) level of theory.

6	-1.439332000	-1.278652000	-0.017810000
6	-1.549827000	0.156181000	0.000814000
7	-0.189411000	-1.867656000	-0.011737000
6	-0.381667000	0.879531000	0.004326000
6	1.002810000	-1.171500000	-0.000718000
6	0.888431000	0.231605000	0.002052000
7	2.139882000	-1.867439000	0.004226000
7	3.264425000	-1.139960000	0.012148000
6	2.152572000	0.872445000	0.013599000
7	3.307896000	0.221809000	0.017863000
6	-2.850807000	0.827011000	-0.000088000
7	-4.032629000	0.265631000	0.386510000
7	-2.998973000	2.106683000	-0.360667000
7	-4.940322000	1.197201000	0.271981000
7	-4.297971000	2.275230000	-0.170719000
7	-2.338492000	-2.249571000	-0.064969000
7	-1.634405000	-3.409526000	-0.085919000
7	-0.356667000	-3.223359000	-0.055087000
7	2.172130000	2.261645000	0.020396000
7	3.306934000	2.800256000	0.029035000

7	4.242624000	3.432839000	0.036925000
8	4.342548000	-1.729708000	0.015525000
1	-0.415784000	1.962466000	0.013641000
1	-4.772813000	3.148997000	-0.360784000

Combustion details:

Results of the calculation of **compound 5**.

Reactant information:

JMK273N, 100 %

C(7.000) H(3.000) N(11.000) O(2.000)

Molecular weight = 273.18

Theoretical maximum density = 1.83 g/cm3

Density = 1.83 g/cm3 (100.00 % TMD)

Initial pressure = 0.1 MPa

Oxygen balance = -79.0638 %

Enthalpy of formation = 2731.17 kJ/kg (746.10 kJ/mol)

Energy of formation = 2803.76 kJ/kg (765.93 kJ/mol)

Detonation parameters (at the C-J point) :

Heat of detonation = -3727.322 kJ/kg

Detonation temperature = 2594.385 K

Detonation pressure = 22.98748 GPa

Detonation velocity = 7793.52 m/s

Particle velocity = 1611.777 m/s

Sound velocity = 6181.743 m/s

Exponent 'Gamma' = 3.835343

Density of all products = 2.307139 g/cm3

Density of gaseous products = 2.036859 g/cm3

Specific volume of all products = 0.4334372 cm3/g

Specific volume of gaseous products = 0.4909519 cm3/g

Volume of gas at STP = **582.542 L/kg**

Moles of gaseous products = 25.99 mol/kg

Moles of condensed products = 23.7 mol/kg

Mean molecular mass of gas. prod. = 27.52213 g/mol

Mean molecular mass of cond.prod. = 12.011 g/mol

Mean molecular mass of all prod. = 20.12394 g/mol

Entropy of products = 5.6323 kJ/kg K

Internal energy of products = 5026.245 kJ/kg, i.e. 9.198029 kJ/cm3

Compression energy = 1298.923 kJ/kg, i.e. 2.37703 kJ/cm3

TNT equivalent from Qd = 81.53 %

TNT equivalent from pCJ = 124.89 %

Concentration of detonation products :

(27 products considered)

\---

PRODUCT mol/mol exp. mol/kg expl. Mol % Mass %

\---

C(d) = 6.474464E+00 2.370036E+01 47.6960 28.4665

N_2 = 5.431280E+00 1.988169E+01 40.0111 **55.6946**

H_2O = 9.974198E-01 3.651145E+00 7.3478 6.5776

CH_2O_2 = 2.811269E-01 1.029090E+00 2.0710 4.7364

CO_2 = 1.996795E-01 7.309447E-01 1.4710 3.2169

NH_3 = 1.369463E-01 5.013044E-01 1.0089 0.8538

CO = 4.045117E-02 1.480752E-01 0.2980 0.4148

H_2 = 8.749488E-03 3.202829E-02 0.0645 0.0065

CH_4 = 2.941366E-03 1.076714E-02 0.0217 0.0173

HCNO = 4.598450E-04 1.683304E-03 0.0034 0.0072

H = 4.278251E-04 1.566092E-03 0.0032 0.0002

C_2H_4 = 3.906401E-04 1.429973E-03 0.0029 0.0040

CH_3OH = 5.439717E-05 1.991258E-04 0.0004 0.0006

C_2H_6 = 1.533960E-05 5.615200E-05 0.0001 0.0002

HCN = 1.058739E-05 3.875609E-05 0.0001 0.0001

NH_2 = 7.720620E-06 2.826203E-05 0.0001 0.0000

N_2H_4 = 4.308897E-06 1.577311E-05 0.0000 0.0001

N = 3.617781E-06 1.324321E-05 0.0000 0.0000

N_2O = 2.012551E-06 7.367125E-06 0.0000 0.0000

H_2O_2 = 3.018758E-09 1.105043E-08 0.0000 0.0000

CNO = 2.285962E-09 8.367970E-09 0.0000 0.0000

HNO = 1.848135E-09 6.765266E-09 0.0000 0.0000

CH_2O = 1.542187E-09 5.645314E-09 0.0000 0.0000

NO_2 = 1.364862E-10 4.996202E-10 0.0000 0.0000

HN_3 = 9.241527E-12 3.382944E-11 0.0000 0.0000

NO_3 = 6.336734E-16 2.319619E-15 0.0000 0.0000

C(gr) = 2.922462E-20 1.069793E-19 0.0000 0.0000

Results of the calculation of **compound 8**.

Reactant information:

1. JMK110NB, 100 %

C(7.000) H(2.000) N(14.000) O(1.000)

Molecular weight = 298.2

Theoretical maximum density = 1.8 g/cm3

Density = 1.8 g/cm3 (100.00 % TMD)

Initial pressure = 0.1 MPa

Oxygen balance = -75.11343 %

Enthalpy of formation = 4338.41 kJ/kg (1293.70 kJ/mol)

Energy of formation = 4409.06 kJ/kg (1314.77 kJ/mol)

Detonation parameters (at the C-J point) :

Heat of detonation = -4502.579 kJ/kg

Detonation temperature = 3146.832 K

Detonation pressure = 24.3649 GPa

Detonation velocity = 7934.75 m/s

Particle velocity = 1705.914 m/s

Sound velocity = 6228.835 m/s

Exponent 'Gamma' = 3.651304

Density of all products = 2.292973 g/cm3

Density of gaseous products = 2.038271 g/cm3

Specific volume of all products = 0.4361151 cm3/g

Specific volume of gaseous prod. = 0.4906119 cm3/g

Volume of gas at STP = 596.119 L/kg

Moles of gaseous products = 26.596 mol/kg

Moles of condensed products = 22.417 mol/kg

Mean molecular mass of gas. prod. = 27.47428 g/mol

Mean molecular mass of cond.prod. = 12.011 g/mol

Mean molecular mass of all prod. = 20.4018 g/mol

Entropy of products = 5.8178 kJ/kg K

Internal energy of products = 5957.662 kJ/kg, i.e. 10.72379 kJ/cm3

Compression energy = 1455.083 kJ/kg, i.e. 2.619149 kJ/cm3

TNT equivalent from Qd = 98.49 %

TNT equivalent from pCJ = 132.37 %

Concentration of detonation products :

(27 products considered)

PRODUCT	mol/mol exp.	mol/kg expl.	Mol %	Mass %
N_2 =	6.896235E+00	2.312644E+01	47.1843	**64.7841**
C(d) =	6.684749E+00	2.241722E+01	45.7373	26.9253
H_2O =	4.802991E-01	1.610677E+00	3.2862	2.9017
NH_3 =	2.061670E-01	6.913783E-01	1.4106	1.1775
CH_2O_2 =	1.562585E-01	5.240109E-01	1.0691	2.4118
CO =	8.485223E-02	2.845509E-01	0.5806	0.7970
CO_2 =	6.059948E-02	2.032196E-01	0.4146	0.8944

H_2 = 3.218979E-02 1.079481E-01 0.2202 0.0218

CH_4 = 7.294525E-03 2.446210E-02 0.0499 0.0392

H = 2.973704E-03 9.972279E-03 0.0203 0.0010

C_2H_4 = 2.482736E-03 8.325824E-03 0.0170 0.0234

HCNO = 1.058650E-03 3.550169E-03 0.0072 0.0153

N = 8.927272E-05 2.993750E-04 0.0006 0.0004

NH_2 = 7.750362E-05 2.599074E-04 0.0005 0.0004

HCN = 6.763138E-05 2.268010E-04 0.0005 0.0006

CH_3OH = 6.644407E-05 2.228194E-04 0.0005 0.0007

C_2H_6 = 4.428857E-05 1.485212E-04 0.0003 0.0004

N_2H_4 = 2.720385E-05 9.122776E-05 0.0002 0.0003

N_2O = 7.541290E-06 2.528962E-05 0.0001 0.0001

CNO = 5.754181E-08 1.929657E-07 0.0000 0.0000

HNO = 1.667735E-08 5.592727E-08 0.0000 0.0000

CH_2O = 9.908552E-09 3.322821E-08 0.0000 0.0000

H_2O_2 = 9.782154E-09 3.280433E-08 0.0000 0.0000

NO_2 = 1.093134E-09 3.665812E-09 0.0000 0.0000

HN_3 = 3.203394E-10 1.074254E-09 0.0000 0.0000

NO_3 = 1.436753E-14 4.818133E-14 0.0000 0.0000

C(gr) = 3.375399E-17 1.131936E-16 0.0000 0.0000

Results of the calculation of **NaN_3:**

REACTANT INFORMATION:

1. **Sodium azide (NaN_3)**, 100 %

N(3.000) Na(1.000)

Molecular weight = 65.02

Theoretical maximum density = 1.846 g/cm3

Density = 1.846 g/cm3 (100.00 % TMD)

Initial pressure = 0.1 MPa

Oxygen balance = -12.30408 %

Enthalpy of formation = 326.85 kJ/kg (21.25 kJ/mol)

Energy of formation = 384.04 kJ/kg (24.97 kJ/mol)

Detonation parameters (at the C-J point) :

Heat of detonation = -347.0311 kJ/kg

Detonation temperature = 450.9091 K

Detonation pressure = 12.13266 GPa

Detonation velocity = 6550.084 m/s

Particle velocity = 1003.399 m/s

Sound velocity = 5546.685 m/s

Exponent 'Gamma' = 5.527849

Density of all products = 2.179943 g/cm3

Density of gaseous products = 2.633781 g/cm3

Specific volume of all products = 0.4587277 cm3/g

Specific volume of gaseous prod. = 0.3796822 cm3/g

Volume of gas at STP = 517.127 L/kg

Moles of gaseous products = 23.072 mol/kg

Moles of condensed products = 15.381 mol/kg

Mean molecular mass of gas. prod. = 28.013 g/mol

```
Mean molecular mass of cond.prod. = 22.898  g/mol

Mean molecular mass of all prod.  = 25.967  g/mol

Entropy of products              = 1.6204  kJ/kg K

Internal energy of products       = 850.4443   kJ/kg,  i.e.  1.56992  kJ/cm3

Compression energy               = 503.4132   kJ/kg,  i.e.  0.9293008  kJ/cm3

TNT equivalent from Qd           = 7.95 %

TNT equivalent from pCJ          = 65.37 %
```

Concentration of detonation products :

```
 (4  products considered)

--------------------------------------------------------------------------------

 PRODUCT            mol/mol exp.    mol/kg expl.     Mol %      Mass %

--------------------------------------------------------------------------------

 N2  =            1.500000E+00     2.307160E+01    60.0000    64.6305

 Na(l) =           1.000000E+00     1.538107E+01    40.0000    35.2196

 Na =             8.581673E-12     1.319953E-10     0.0000     0.0000

 N =              0.000000E+00     0.000000E+00     0.0000     0.0000
```

References:

1. Gaussian 09, Revision E.01, M. J.Frisch, G. W. Trucks, H. B. Schlegel, G. E. Scuseria, M A. Robb, J. R. Cheeseman, G. Scalmani, V. Barone, B. Mennucci, G. A. Petersson, H. Nakatsuji, M Caricato, X. Li, H. P. Hratchian, A. F. Izmaylov, J. Bloino, G. Zheng, J. L. Sonnenberg, M. Hada, M. Ehara, K. Toyota, R. Fukuda, J. Hasegawa, M. Ishida, T. Nakajima, Y. Honda, O. Kitao, H. Nakai, T. Vreven, Jr. J. A. Montgomery, J. E. Peralta, F. Ogliaro, M. Bearpark, J. J. Heyd, E. Brothers, K. N. Kudin, V. N. Staroverov, R. Kobayashi, J. Normand, K. Raghavachari, A. Rendell, J. C. Burant, S. S. Iyengar, J. Tomasi, M. Cossi, N. Rega, J. M. Millam, M. Klene, J. E. Knox, J. B. Cross, V. Bakken, C. Adamo, J. Jaramillo, R. Gomperts, R. E. Stratmann, O. Yazyev, A. J. Austin, R. Cammi, C. Pomelli, J. W. Ochterski, R. L. Martin, K. Morokuma, V. G. Zakrzewski,

G. A. Voth, P. Salvador, J. J. Dannenberg, S. Dapprich, A. D. Daniels, O. Farkas, J. B. Foresman, J. V. Ortiz, J. Cioslowski, D. J. Fox, *Gaussian*, Inc., Wallingford CT, 2013.

2. P. Politzer, Y. Ma, P. Lane, M. C. Concha, *Int. J. Quant. Chem.*, 2005, **105**, 341-347.
3. T. Lu, F. Chen, *J. Comput. Chem.*, 2012, **3**, 580–592.
4. A. Woiczechowski-Pop, R. A. Varga, A. Terec and I. Grosu, *Acta. Crystallogr. Sect. E. Struct. Rep. Online.*, 2010, **66**, o2638-o2638.
5. X. Wang, J. Li and Y. Hayashi, *Chem. Commun.,* 2021,**57**, 4283-4286.
6. Y.H. Joo, and J. M. Shreeve, *Eur. J. Org. Chem.*, 2009, **2009**, 3573-3578.
7. L. Bauer, M. Benz, T. M. Klapötke, C. Pignot and J. Stierstorfer, *Mater. Adv.,* 2022, **3**, 3945-3951.
8. M. Kofen, M. Lommel, M. H. H. Wurzenberger, T. M. Klapötke and J. Stierstorfer, *Chem. Eur. J.*, 2022, **28**, e202200492.
9. D. Izsák, T. M. Klapötke and C. Pflüger, *Dalton Trans.*, 2015, **44**, 17054-17063.
10. F. A. Bulat, A. Toro-Labbé, T. Brinck, J. S. Murray and P. Politzer, *J. Mol. Model,* 2010, **16**, 1679-1691.
11. J. S. Murray and P. Politzer, *Wiley Interdiscip. Rev. Comput. Mol. Sci.*, 2017, **7**, e1326.
12. M. T. Ibrahim, M. M. Ibrahim, A. Uzairu, G. A. Shallangwa and S. Uba, *Discover Chem*, 2025, **2**, 1-17.
13. K. Sharma, A. Maan, V. D. Ghule and S. Dharavath, *J. Phys. Chem. A.*, 2023, **127**, 10128-10138.